

# Modal Gating of Human Ca<sub>v</sub>2.1 (P/Q-type) Calcium Channels: I. The Slow and the Fast Gating Modes and their Modulation by $\beta$ Subunits

SIRO LUVISETTO,<sup>1</sup> TOMMASO FELLIN,<sup>1</sup> MICHELE SPAGNOLO,<sup>1</sup> BRUNO HIVERT,<sup>1,2</sup> PAUL F. BRUST,<sup>3,4</sup> MICHAEL M. HARPOLD,<sup>3</sup> KENNETH A. STAUDERMAN,<sup>3,5</sup> MARK E. WILLIAMS,<sup>3,6</sup> and DANIELA PIETROBON<sup>1</sup>

<sup>1</sup>Department of Biomedical Sciences and Consiglio Nazionale delle Ricerche Institute of Neuroscience, University of Padova, 35121 Padova, Italy

<sup>2</sup>Department of Biology, Faculte des Sciences de Luminy, 13288 Marseille, cedex 9, France

<sup>3</sup>SIBIA Neurosciences, La Jolla, CA 92037

<sup>4</sup>Senomyx Inc., La Jolla, CA 92037

<sup>5</sup>Neurogenetics Inc., La Jolla, CA 92037

<sup>6</sup>Merck Research Labs, San Diego, CA 92121

**ABSTRACT** The single channel gating properties of human Ca<sub>v</sub>2.1 (P/Q-type) calcium channels and their modulation by the auxiliary  $\beta_{1b}$ ,  $\beta_{2e}$ ,  $\beta_{3a}$ , and  $\beta_{4a}$  subunits were investigated with cell-attached patch-clamp recordings on HEK293 cells stably expressing human Ca<sub>v</sub>2.1 channels. These calcium channels showed a complex modal gating, which is described in this and the following paper (Fellin, T., S. Luvisetto, M. Spagnolo, and D. Pietrobon. 2004. *J. Gen. Physiol.* 124:463–474). Here, we report the characterization of two modes of gating of human Ca<sub>v</sub>2.1 channels, the slow mode and the fast mode. A channel in the two gating modes differs in mean closed times and latency to first opening (both longer in the slow mode), in voltage dependence of the open probability (larger depolarizations are necessary to open the channel in the slow mode), in kinetics of inactivation (slower in the slow mode), and voltage dependence of steady-state inactivation (occurring at less negative voltages in the slow mode). Ca<sub>v</sub>2.1 channels containing any of the four  $\beta$  subtypes can gate in either the slow or the fast mode, with only minor differences in the rate constants of the transitions between closed and open states within each mode. In both modes, Ca<sub>v</sub>2.1 channels display different rates of inactivation and different steady-state inactivation depending on the  $\beta$  subtype. The type of  $\beta$  subunit also modulates the relative occurrence of the slow and the fast gating mode of Ca<sub>v</sub>2.1 channels;  $\beta_{3a}$  promotes the fast mode, whereas  $\beta_{4a}$  promotes the slow mode. The prevailing mode of gating of Ca<sub>v</sub>2.1 channels lacking a  $\beta$  subunit is a gating mode in which the channel shows shorter mean open times, longer mean closed times, longer first latency, a much larger fraction of nulls, and activates at more positive voltages than in either the fast or slow mode.

**KEY WORDS:** Ca<sup>2+</sup> channel • gating mode • synaptic transmission • familial hemiplegic migraine • auxiliary subunit

## INTRODUCTION

Voltage-gated P/Q-type calcium channels (Ca<sub>v</sub>2.1) are located in presynaptic terminals and somatodendritic membranes throughout the brain (Volsen et al., 1995; Westenbroek et al., 1995), and have a prominent role in controlling neurotransmitter release (Dunlap et al., 1995). The somatodendritic localization of Ca<sub>v</sub>2.1 channels points to additional postsynaptic roles in, for example, neural excitability (Bayliss et al., 1997; Pineda et al., 1998; Mori et al., 2000), synaptic integration and plasticity (Eilers et al., 1996; Magee et al., 1998), and gene expression (Sutton et al., 1999). The importance of Ca<sub>v</sub>2.1 channels in brain function is stressed by the evidence that mutations in CACNA1A, the gene encoding Ca<sub>v</sub>2.1 $\alpha_1$  subunits, cause a group of domi-

nantly inherited human neurological disorders, including familial hemiplegic migraine, episodic ataxia type-2, and spinocerebellar ataxia type 6 (Ophoff et al., 1996; Zhuchenko et al., 1997). Mutations at the mouse orthologue cause a group of recessive neurological disorders, including the *tottering*, *leaner*, and *rocker* phenotypes with ataxia and absence epilepsy, and the *rolling Nagoya* phenotype with ataxia without seizures (Fletcher et al., 1996; Pietrobon, 2002). In the *lethargic* mouse, a mutation in the gene encoding the auxiliary calcium channel  $\beta_4$  subunit causes a clinical phenotype very similar to that of *tottering* (Burgess et al., 1997). Knockout mice with a null mutation in the Ca<sub>v</sub>2.1 $\alpha_1$  gene show severe cerebellar ataxia and dystonia and selective progressive cerebellar degeneration (Jun et al., 1999; Fletcher et al., 2001).

The single channel gating properties of Ca<sub>v</sub>2.1 channels are critical determinants of the time course

Address correspondence to Daniela Pietrobon, Dept. of Biomedical Sciences, University of Padova, Viale G. Colombo 3, 35121 Padova, Italy. Fax: 39-049-8276049. email: daniela.pietrobon@unipd.it

Abbreviation used in this paper: HEK, human embryonic kidney.

and magnitude of the various  $\text{Ca}^{2+}$ -dependent processes they control. Both experiments and simulations have shown that even small changes in the kinetics of channel opening and/or closing and in channel open probability can strongly affect the time course and magnitude of  $\text{Ca}^{2+}$  influx during an action potential (McCobb and Beam, 1991; Borst and Sakmann, 1998; Sabatini and Regehr, 1999; Colecraft et al., 2001; Bischofberger et al., 2002; Meinrenken et al., 2002, 2003). Given the steep dependence of neurotransmitter release on  $\text{Ca}^{2+}$  influx (Dodge and Rahamimoff, 1967; Bollmann et al., 2000; Schneggenburger and Neher, 2000), the detailed gating properties of single  $\text{Ca}_v2.1$  channels will have a strong impact especially on the time course and magnitude of neurotransmitter release at central synapses, where P/Q channels appear to be more effectively coupled to release than other  $\text{Ca}^{2+}$  channel types (Mintz et al., 1995; Wu et al., 1999; Qian and Noebels, 2001). Despite the critical role of  $\text{Ca}_v2.1$  channel gating in determining neurotransmission efficacy at central synapses, surprisingly few data are available on the single channel gating properties of native P/Q-type  $\text{Ca}^{2+}$  channels (Usovich et al., 1992; Forti et al., 1994; Tottene et al., 1996) or recombinant  $\text{Ca}_v2.1$  channels (Yatani et al., 1994; Bourinet et al., 1999; Hans et al., 1999; Colecraft et al., 2001; Tottene et al., 2002). The discovery that mutations causing familial hemiplegic migraine increase the open probability and the single channel  $\text{Ca}^{2+}$  influx through human  $\text{Ca}_v2.1$  channels (Hans et al., 1999; Tottene et al., 2002) and, as a consequence, facilitate the induction and the propagation of cortical spreading depression (van den Maagdenberg et al., 2004) fosters the interest in extending our knowledge of the single channel properties of human  $\text{Ca}_v2.1$  channels. Therefore, one of our aims here was to obtain a detailed characterization of the gating properties of human  $\text{Ca}_v2.1$  channels at the single channel level.

In heterologous expression systems,  $\beta$  subunits are powerful regulators of both channel activity and number of channels expressed in the membrane (Walker et al., 1998; Dolphin, 2003a). In particular, for the  $\text{Ca}_v2.1$  channel, there is evidence for both a chaperone-like effect of  $\beta$  subunits on channel trafficking to the plasma membrane (Brice et al., 1997; Bichet et al., 2000) and modulation of the voltage range of activation and inactivation as well as the kinetics of inactivation of the whole-cell current (Stea et al., 1994; De Waard and Campbell, 1995; De Waard et al., 1995; Cens et al., 1996). Four different genes encode  $\beta$  subunits ( $\beta_{1,2,3,4}$ ) that are differentially expressed in different neurons and during development (Tanaka et al., 1995; Witcher et al., 1995; Ludwig et al., 1997; Volsen et al., 1997; Vance et al., 1998; Burgess et al., 1999). Regional differences in brain expression pattern can also occur for

splice variants of the same  $\beta$  subunit (Helton et al., 2002). Native P/Q-type channels can contain each of the four different  $\beta$  subunits (Liu et al., 1996), and the fractional contribution of a particular  $\beta$  subunit for channel formation varies among different brain regions (Pichler et al., 1997). Different combinations of a  $\text{Ca}_v2.1\alpha_1$  subunit with auxiliary  $\beta$  subunits most likely contribute to generate the large functional diversity of native P/Q-type calcium channels (Mintz et al., 1992; Usovich et al., 1992; Randall and Tsien, 1995; Tottene et al., 1996; Forsythe et al., 1998; Mermelstein et al., 1999). Whole-cell current recordings in heterologous expression systems revealed quite different kinetics of inactivation and slightly different voltage ranges of activation depending on the  $\beta$  subtype combined with the  $\text{Ca}_v2.1\alpha_1$  subunit (Sather et al., 1993; Stea et al., 1994; De Waard and Campbell, 1995; De Waard et al., 1995; Cens et al., 1996; Moreno et al., 1997; Krovetz et al., 2000; Restituito et al., 2000; Sokolov et al., 2000; Sandoz et al., 2001; Helton and Horne, 2002; Helton et al., 2002; Tsunemi et al., 2002). However, the effect of different  $\beta$  subunits on the single channel gating properties of  $\text{Ca}_v2.1$  channels (and also of the other  $\text{Ca}_v$  channels, with the exception of  $\text{Ca}_v1.2$ ) remains unknown. Interestingly, distinct  $\beta$  subunits confer unique single channel gating properties to L-type channels extending well beyond differences in inactivation (Colecraft et al., 2002). The regulation of  $\text{Ca}_v2.1$  channel properties by variations in  $\beta$  subunit composition appears as a potential mechanism for tuning channel behavior to support a given physiological role, and might contribute to create the great diversity of release efficacy and short-term synaptic plasticity at different synapses (Atwood and Karunanithi, 2002). Therefore a second aim here is to study how the presence of different auxiliary  $\beta$  subunits in the human  $\text{Ca}_v2.1$  channel alters gating at the single channel level.

Single channel patch-clamp recordings on human embryonic kidney HEK293 cells expressing human  $\text{Ca}_v2.1$  channels revealed a complex modal gating of these channels, which is described in this and the accompanying paper (Fellin et al., 2004). Here, we report the characterization of two modes of gating of human  $\text{Ca}_v2.1$  channels, the slow mode and the fast mode, that differ in mean closed times and latency to first opening, in voltage dependence of the open probability, in kinetics of inactivation, and voltage dependence of steady-state inactivation. The study of  $\text{Ca}_v2.1$  channels containing four different  $\beta$  subunits shows that both the relative occurrence of the slow and fast gating modes and the inactivation properties within each mode are modulated by the type of  $\beta$  subunit. We also show that the prevailing mode of gating of  $\text{Ca}_v2.1$  channels lacking a  $\beta$  subunit is a low- $p_o$  mode different from both the fast and the slow gating modes.

### Cell Culture and Transfection

HEK293 cells (American Type Culture Collection, CRL-1533) were stably transfected with cDNA constructs encoding the human  $\text{Ca}_v2.1\alpha_1$  ( $\alpha_{1A-2}$ ),  $\alpha_{2b}\delta$ -1, and  $\beta_{1b}$  (A68-90 cell line) or  $\beta_{2c}$  (EIH2 cell line) or  $\beta_{3a}$  (PB1-14 cell line) or  $\beta_{4a}$  (10-13 cell line) subunits using a standard calcium phosphate-mediated procedure (Hans et al., 1999). Antibiotic-resistant colonies were selected in medium consisting of Dulbecco's modified Eagle's medium (DMEM; Life Technologies) supplemented with 6% bovine calf serum, penicillin, streptomycin, and G418 or a combination of G418 and Zeocin depending on the constructs used. Cells were maintained on standard tissue culture plates at 37°C and 5%  $\text{CO}_2$ . Parental lines and subsequent subclones were selected based on the following criteria: (a) functional responses in a fluo3 dye-based assay where increases in intracellular  $\text{Ca}^{2+}$  are measured in response to KCl depolarization; (b) Northern and Western analysis, and (c) electrophysiological characterization. All cell lines were incubated at 28°C for 12–24 h before electrophysiological measurements (and in the case of the PB1-14 cell line also before the fluo3 assay) (Hans et al., 1999).

In the case of transient transfection of HEK293 cells with cDNA constructs encoding the human  $\text{Ca}_v2.1\alpha_1$  ( $\alpha_{1A-2}$ ) and  $\alpha_{2b}\delta$ -1 subunits (or of PB1-14 cells with cDNA constructs encoding the  $\beta_{3a}$  subunit), CD4 expression plasmids were included to permit the identification of transfected cells as in Hans et al. (1999).

In untransfected HEK293 cells, neither  $\text{Ca}_v2.1\alpha_1$  nor  $\beta$  transcripts were detected by Northern blots and neither  $\text{Ca}_v2.1\alpha_1$  nor  $\beta$  protein was detected on Western blots (not depicted). In contrast, both Northern and Western blot assays revealed the presence of an endogenous  $\alpha_{2b}\delta$ -1 subunit in the same cells (not depicted).

### Patch-clamp Recordings and Data Analysis

Single channel patch-clamp recordings were performed following standard techniques, as in Hans et al. (1999). Currents were recorded at room temperature with a DAGAN 3900 patch-clamp amplifier, low-pass filtered at 1 kHz (–3 dB, 8-pole Bessel filter), sampled at 5 kHz, and stored for later analysis on a PDP-11/73 computer. All single channel recordings were obtained in the cell-attached configuration. The pipette solution contained (in mM) 90  $\text{BaCl}_2$ , 10 TEA-Cl, 15 CsCl, 10 HEPES (pH 7.4 with TEA-OH). The bath solution contained (in mM) 140 K-gluconate, 5 EGTA, 35 l-glucose, 10 HEPES (pH 7.4 with KOH). The high-potassium bath solution was used to zero the membrane potential outside the patch. Liquid junction potential at the pipette tip was +12 mV, and this value should be subtracted from all voltages to obtain correct values of membrane potentials.

Linear leak and capacitive currents were digitally subtracted from all records used for analysis. Open-channel current amplitudes were measured by manually fitting cursors to well-resolved channel openings. Values at each voltage are averages of many measurements. Open probability,  $p_o$ , was computed by measuring the average current,  $\langle I \rangle$ , in a given single channel current record and dividing it by the unitary single channel current,  $i$ . To obtain activation curves,  $p_o$  values were calculated in patches containing only one channel by averaging the open probabilities measured in each sweep with activity at a given voltage (excluding the last shut time). Single channel activation curves were best fitted with the Boltzmann equation  $p_o = p_{o\max} \times [1 + \exp\{-(V - V_{1/2})/k\}]^{-1}$ , where  $k = RT/zF$ . For open and closed time histograms, a channel opening or closure was detected when more than one sampling point crossed a discriminator line at 50% of the elementary current. Histograms of open and closed times

were fitted with sums of decaying exponentials. Log binning and fitting of the binned distributions were done as described by McManus et al. (1987) and Sigworth and Sine (1987). The first closed time was used to generate the cumulative first latency histogram. The best fit was determined by the maximum likelihood maximization (Colquhoun and Sigworth, 1983), and the best minimum number of exponential components was determined by the maximum likelihood ratio test (Rao, 1973). All values are given as mean  $\pm$  SEM.

## RESULTS

Cell-attached single channel recordings on HEK293 cells stably coexpressing human  $\text{Ca}_v2.1\alpha_1$  ( $\alpha_{1A-2}$ ),  $\beta_{1b}$ , and  $\alpha_{2b}\delta$ -1 subunits revealed that, in many patches containing only one channel, the same channel showed two different modes of gating. Fig. 1 A shows consecutive traces from a single channel patch displaying activity of the same  $\text{Ca}_v2.1$  channel in two different periods at the same voltage (+30 mV). Analysis of the open and closed time histograms in the two periods shows that the two modes of gating differ mainly in the intervals of time spent by the channel in closed states (Fig. 1 B and Fig. 2 A). We have called these two modes of gating “slow” and “fast” for reasons that will become clear below, when the kinetics of inactivation and the latencies to first opening of a  $\text{Ca}_v2.1$  channel in the two modes will be considered.

The transitions between the two modes were infrequent. The channel shown in Fig. 1 was in the slow gating mode during the first 8 min of the recording, and then switched to the fast mode and remained in this gating mode until the end of the recording (for almost 40 min). In different single channel patches, the intervals of time spent by the channel in each gating mode varied from tens of seconds to tens of minutes. Average values of the different gating parameters for the two gating modes in isolation were obtained from single channel patches in which, by visual inspection, the channel showed only (or mainly) one gating mode or two clearly separated periods in the two modes (Fig. 2 A).

In both gating modes, open and closed time histograms were best fit by the sum of two and three exponential components, respectively. Both the time constants and the relative areas of the two exponential components best fitting the open time histograms were similar for the two gating modes, whereas two of the closed time constants ( $\tau_{c2}$  and  $\tau_{c3}$ ) were significantly larger in the slow mode than in the fast mode (Fig. 1 B and Fig. 2 A). Moreover, their relative areas were different in the two gating modes, showing a larger contribution of the longest closed time intervals in the slow with respect to the fast gating mode. As a result, at +30 mV, the open probability of the channel in the fast gating mode was about twice that in the slow mode (Fig. 1 C and Fig. 2 B). Measurements of the open probability,  $p_o$ , as a function of voltage revealed that the  $\text{Ca}_v2.1$

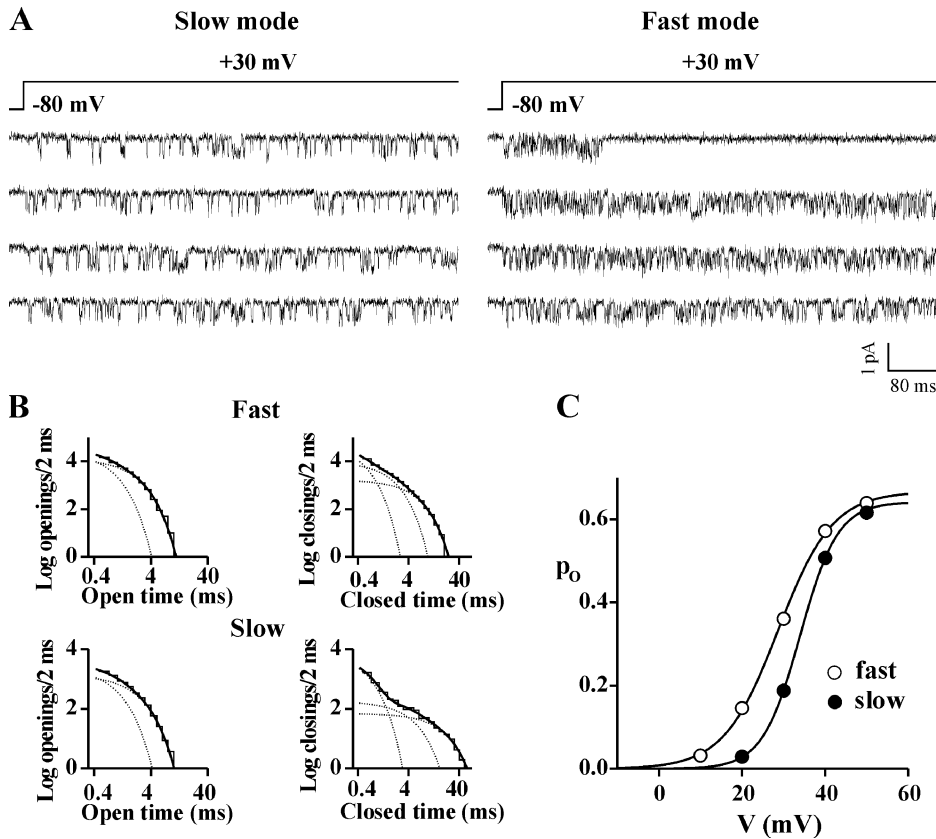


FIGURE 1. A single human  $\text{Ca}_v2.1$  channel shows two different modes of gating: the fast and slow modes. Cell-attached single channel recordings with 90 mM  $\text{Ba}^{2+}$  as charge carrier on HEK293 cells stably coexpressing human  $\text{Ca}_v2.1\alpha_1$  ( $\alpha_{1A-2}$ ),  $\beta_{1b}$  and  $\alpha_{2b}\delta$ -1 subunits. Depolarizations were 720 ms long and were delivered every 4 s from a holding potential of  $-80$  mV. Records were sampled and filtered at 5 and 1 kHz, respectively. (A) Consecutive traces in two different periods from a patch containing a single  $\text{Ca}_v2.1$  channel. By visual inspection, the channel was in the mode of gating shown on the left (the slow gating mode) during the first 8 min of recording, and in the mode of gating shown on the right (the fast gating mode) during the remaining 40 min. Single channel current and conductance were identical in the two periods. (B) Log-log plots of the open and closed time distributions of the same single channel in the two periods in fast and slow gating mode. The dark solid line in each plot is the best-fitting sum of two or three exponential components for the open or closed times, respectively (each exponential component is shown as a dotted

line); time constants of the open times: 0.54 and 1.42 ms (relative areas 40 and 60%) for the slow mode and 0.40 and 1.36 ms (relative areas 71 and 29%) for the fast mode; time constants of the closed times: 0.34, 3.17, and 13.4 ms (relative areas 64, 14, and 22%) for the slow mode, and 0.29, 1.17, and 3.54 ms (relative areas 43, 38, and 19%) for the fast mode. (C) Open probability,  $p_o$ , as a function of voltage for the same single channel gating in the fast (empty symbol) and slow (dark symbol) mode. Fit of the two activation curves with a Boltzmann equation gives  $V_{1/2} = 34$  mV,  $k = 4.5$  mV, and  $p_{o,max} = 0.64$  for the slow mode and  $V_{1/2} = 29$  mV,  $k = 6.6$  mV, and  $p_{o,max} = 0.67$  for the fast mode. The companion paper (Fellin et al., 2004) describes two additional modes of gating of  $\text{Ca}_v2.1$  channels named b and nb modes; the single channel shown here was in the nb mode for the entire duration of the recording.

channel activates at more negative voltages in the fast gating mode than in the slow mode (Fig. 1 C and Fig. 2 B). Fit with a Boltzmann function of the average activation curve of  $\text{Ca}_v2.1$  channels containing the  $\beta_{1b}$  subunit gave  $V_{1/2}$  values of 25 and 32 mV (with  $k$  values of 5.3 and 4.2 mV) for the fast and slow gating mode, respectively. The single channel currents and conductance were identical in the two gating modes (not depicted, c.f. Table I).

The fast and slow modes of gating were observed in cells coexpressing human  $\alpha_{1A-2}$ ,  $\alpha_{2b}\delta$ -1, and any of the four different  $\beta$  subunits. Fig. 2 B shows that the activation curves of single channels containing either  $\beta_{1b}$ , or  $\beta_{2e}$ , or  $\beta_{4a}$  subunits in the fast gating mode were similarly shifted to more negative voltages with respect to the corresponding channels in the slow mode. Fits with Boltzmann distributions gave  $V_{1/2}$  values of 28 and 27 mV for channels containing either  $\beta_{2e}$  or  $\beta_{4a}$  subunits in the fast gating mode (with  $k$  values of 6.6 and 5 mV), and  $V_{1/2}$  values of 36 and 34 mV for the corresponding

channels in the slow gating mode (with  $k$  values of 5.9 and 4 mV). The average activation curve of channels containing the  $\beta_{3a}$  subunit in the fast gating mode was similar to that of channels containing the other  $\beta$  subunits ( $V_{1/2} = 23$  mV,  $k = 3.7$ ,  $n = 6$ , not depicted; the only significant difference was with respect to the  $V_{1/2}$  value of channels containing the  $\beta_{2e}$  subunit). An average activation curve in the slow gating mode is not available, given the relatively low occurrence of that gating mode in channels containing the  $\beta_{3a}$  subunit (see below).

Single channels containing the different  $\beta$  subunits in either the fast or the slow gating mode had similar open and closed time histograms at  $+30$  mV, as shown by the average values of the open and closed time constants in Table I. Only the channels with the  $\beta_{2e}$  subunit displayed some significant difference with respect to those with the  $\beta_{1b}$  subunit, and, precisely, both  $\tau_{c2}$  and  $\tau_{c3}$  in the slow gating mode were larger ( $P < 0.05$ ). As a consequence, the open probability at  $+30$  mV in the

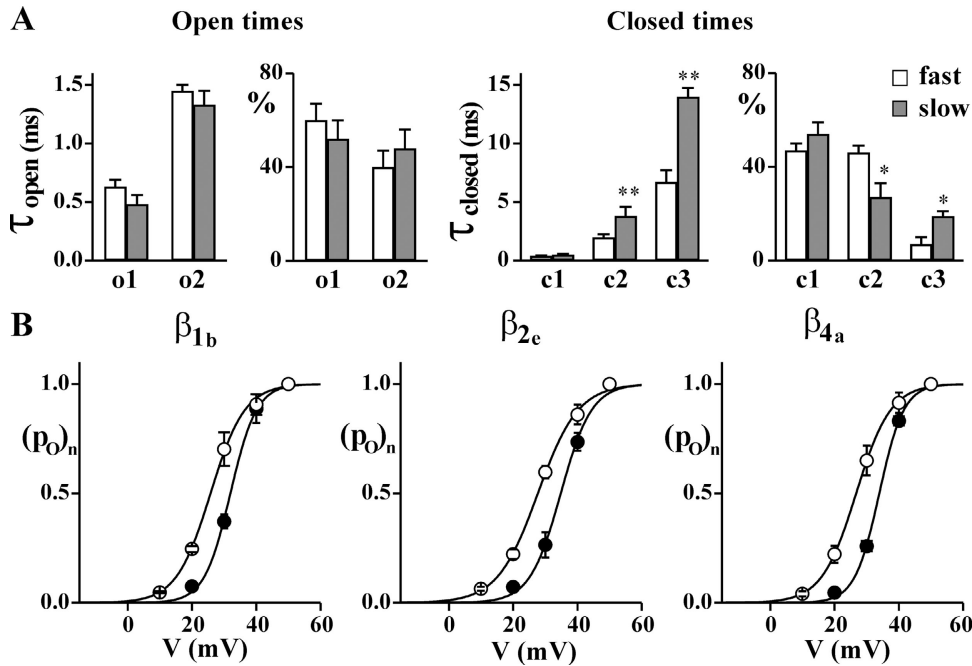


FIGURE 2. A single human  $Ca_v2.1$  channel in the slow gating mode spends longer intervals of time in closed states and activates at more positive voltages than in the fast gating mode. Single channel recordings as in Fig. 1 on HEK293 cells stably coexpressing human  $Ca_v2.1\alpha_1$  ( $\alpha_{1A-2}$ ),  $\alpha_{2b}\delta-1$ , and  $\beta_{1b}$ ,  $\beta_{2c}$ , or  $\beta_{4a}$  subunits. (A) Time constants ( $\tau_{open}$  and  $\tau_{closed}$ ) and relative areas (%) of the exponential components best fitting the open and closed time distributions at +30 mV of single  $Ca_v2.1$  channels ( $\alpha_{1A-2}-\beta_{1b}-\alpha_{2b}\delta-1$ ) in the slow (dark bar) and the fast (empty bar) gating mode. Average values were obtained from single channel patches ( $n = 5$  for both the slow and fast mode) in which, by visual inspection, the channel showed only (or mainly) one gating mode or two clearly separated periods in the two

modes. Average single channel current and conductance were identical for the five channels in either the slow or fast gating mode. Statistical significance of difference between paired values using student  $t$  test: \*,  $P < 0.05$ ; \*\*,  $P < 0.001$ . (B) Normalized open probability,  $p_o$ , as a function of voltage of single  $Ca_v2.1$  channels containing different  $\beta$  subunits gating in the fast (empty symbol) and the slow mode (dark symbol). Average values were obtained from single channel patches in which the channel showed only (or mainly) one gating mode or two clearly separated periods in the two modes:  $n = 5, 5$ , and 6 for the slow mode and  $n = 5, 4$ , and 4 for the fast mode of channels containing the  $\beta_{1b}$ ,  $\beta_{2c}$ , and  $\beta_{4a}$  subunits, respectively.

slow gating mode was smaller with the  $\beta_{2c}$  than with the  $\beta_{1b}$  subunit ( $P < 0.05$ ).

Overall, from the data in Table I and Fig. 2, we can conclude that channels containing different  $\beta$  subunits

in either the fast or the slow gating mode show only minor differences in the rate constants of the transitions between closed and open states within each gating mode.

TABLE I

Single Human  $Ca_v2.1$  Channels Containing Different  $\beta$  Subunits Have Similar Open and Closed Time Distributions in Either the Fast or the Slow Mode of Gating

	$\tau_{o1}$	$\tau_{o2}$	$\tau_{c1}$	$\tau_{c2}$	$\tau_{c3}$	$p_o$	$i$	$n$
Fast mode								
$\beta_{1b}$	$0.63 \pm 0.06$	$1.4 \pm 0.1$	$0.39 \pm 0.05$	$2.0 \pm 0.3$	$6.7 \pm 1.0$	$0.350 \pm 0.020$	$0.76 \pm 0.01$	5
$\beta_{2c}$	$0.54 \pm 0.03$	$1.2 \pm 0.1$	$0.45 \pm 0.02$	$2.4 \pm 0.2$	$7.4 \pm 0.5$	$0.284 \pm 0.013^a$	$0.75 \pm 0.01$	3
$\beta_{3a}$	$0.65 \pm 0.12$	$1.5 \pm 0.2$	$0.41 \pm 0.04$	$2.1 \pm 0.2$	$6.2 \pm 0.3$	$0.330 \pm 0.014$	$0.74 \pm 0.01$	6
$\beta_{4a}$	$0.47 \pm 0.08$	$1.4 \pm 0.04$	$0.33 \pm 0.03$	$2.0 \pm 0.3$	$6.4 \pm 0.9$	$0.308 \pm 0.040$	$0.73 \pm 0.01$	4
Slow mode								
$\beta_{1b}$	$0.48 \pm 0.08$	$1.3 \pm 0.1$	$0.49 \pm 0.08$	$3.8 \pm 0.8$	$14 \pm 1$	$0.188 \pm 0.012$	$0.76 \pm 0.01$	5
$\beta_{2c}$	$0.48 \pm 0.03$	$1.3 \pm 0.1$	$0.56 \pm 0.04$	$7.2 \pm 2.0^b$	$24 \pm 4^c$	$0.125 \pm 0.021^c$	$0.73 \pm 0.03$	4
$\beta_{4a}$	$0.56 \pm 0.12$	$1.6 \pm 0.2$	$0.38 \pm 0.07$	$2.2 \pm 0.8$	$18 \pm 4$	$0.150 \pm 0.024$	$0.73 \pm 0.02$	4

Single channel recordings as in Fig. 1 on HEK293 cells stably coexpressing human  $Ca_v2.1\alpha_1$  ( $\alpha_{1A-2}$ ),  $\alpha_{2b}\delta-1$ , and  $\beta_{1b}$ ,  $\beta_{2c}$ ,  $\beta_{3a}$ , or  $\beta_{4a}$  subunits. Time constants of the exponential components best fitting the open ( $\tau_{o1}$  and  $\tau_{o2}$ ) and closed ( $\tau_{c1}$ ,  $\tau_{c2}$ , and  $\tau_{c3}$ ) time distributions at +30 mV of single  $Ca_v2.1$  channels containing different  $\beta$  subunits in slow and fast gating modes. Average values were obtained from single channel patches in which the channel showed only (or mainly) one gating mode or two clearly separated periods in the two modes. Average values of the open probability and the unitary current from the same patches are also shown. Most of the data for  $Ca_v2.1$  channels containing the  $\beta_{3a}$  subunit were obtained from PB1-14 cells transfected with  $\beta_{3a}$  cDNA (given the low level of expression of  $\beta_{3a}$  subunit in this stable cell line).

<sup>a</sup> $\beta_{2c}$  with respect to  $\beta_{1b}$  and  $\beta_{3a}$ ,  $P < 0.05$ .

<sup>b</sup> $\beta_{2c}$  with respect to  $\beta_{1b}$  and  $\beta_{4a}$ ,  $P < 0.05$ .

<sup>c</sup> $\beta_{2c}$  with respect to  $\beta_{1b}$ ,  $P < 0.05$ .

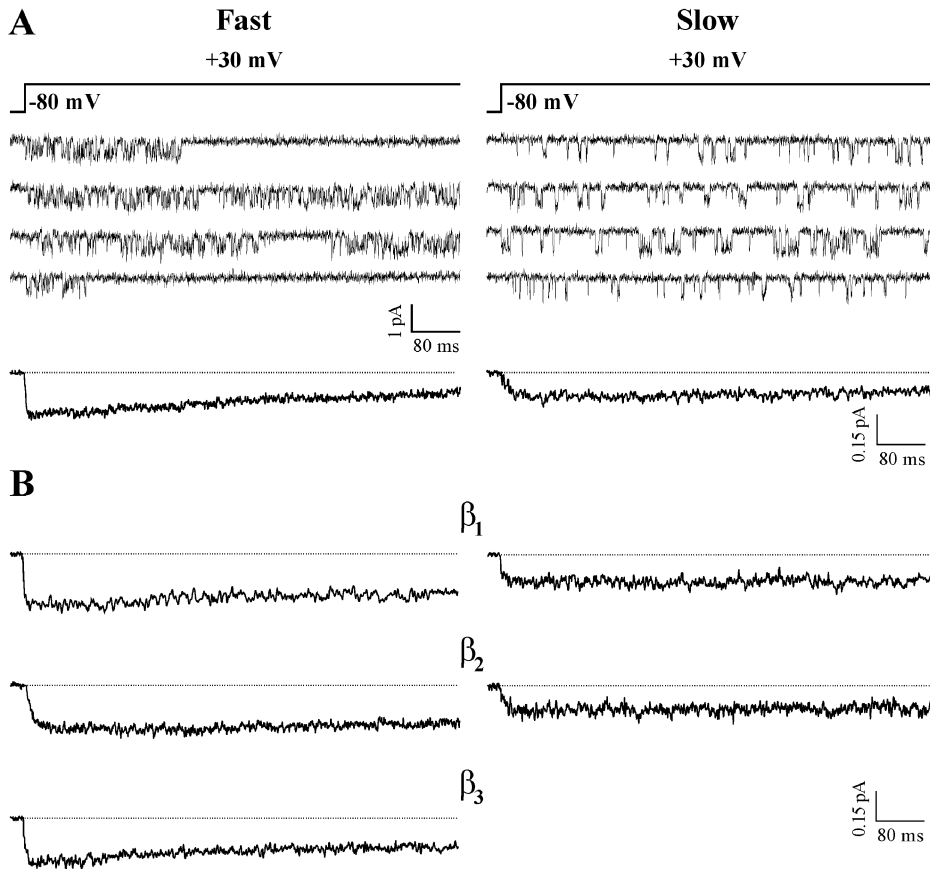


FIGURE 3. A single human  $\text{Ca}_v2.1$  channel in the fast gating mode inactivates more rapidly than in the slow gating mode, independently of the  $\beta$  subtype. Single channel recordings as in Fig. 1 on HEK293 cells stably coexpressing human  $\text{Ca}_v2.1\alpha_1$  ( $\alpha_{1A-2}$ ),  $\alpha_{2\delta-1}$ , and  $\beta_{4a}$ ,  $\beta_{1b}$ ,  $\beta_{2c}$ , and  $\beta_{3a}$  subunits. (A) Representative traces at +30 mV from two patches containing a single  $\text{Ca}_v2.1$  ( $\alpha_{1A-2}\beta_{4a}\alpha_{2\delta-1}$ ) channel in either the fast (left) or the slow gating mode (right), and pooled average single channel ensemble currents at +30 mV from five ( $n = 323$  traces) and four patches ( $n = 213$  traces) containing a single channel in the fast and slow gating mode, respectively. (B) Pooled average single channel ensemble currents at +30 mV of  $\text{Ca}_v2.1$  channels containing different  $\beta$  subunits gating in either the fast (left) or slow mode (right). Fast mode:  $\beta_{1b}$ ,  $n = 133$  from three patches;  $\beta_{2c}$ ,  $n = 301$  from four patches;  $\beta_{3a}$ ,  $n = 201$  from five patches. Slow mode:  $\beta_{1b}$ ,  $n = 139$  from three patches;  $\beta_{2c}$ ,  $n = 163$  from three patches. Average ensemble currents were obtained from single channel patches in which, by visual inspection, the channel showed only (or mainly) one gating

mode or two clearly separated periods in the two modes. Most of the data for  $\text{Ca}_v2.1$  channels containing the  $\beta_{3a}$  subunit were obtained from PBI-14 cells transfected with  $\beta_{3a}$  cDNA. The fraction of peak current remaining after 720 ms was 49, 72, 86, and 66% for channels in the fast mode with  $\beta_{4a}$ ,  $\beta_{1b}$ ,  $\beta_{2c}$ , and  $\beta_{3a}$ , respectively, and 89, 100, and 100% for channels in slow mode with  $\beta_{4a}$ ,  $\beta_{1b}$ , and  $\beta_{2c}$ , respectively.

In addition to different properties of activation, the human  $\text{Ca}_v2.1$  channel showed different properties of inactivation in the two modes of gating (Figs. 3 and 4). During depolarizations to +30 mV, lasting 720 ms, single channels containing the  $\beta_{4a}$  subunit showed both inactivating and noninactivating activity in the fast gating mode, but almost exclusively noninactivating activity in the slow mode (Fig. 3 A). Thus, as shown by the average single channel ensemble currents, inactivation was more rapid in the fast than in the slow gating mode. The kinetics of inactivation were more rapid in the fast than in the slow gating mode independently of the type of  $\beta$  subunit combined with the  $\text{Ca}_v2.1\alpha_1$  subunit (Fig. 3 B). However, the kinetics of inactivation in each gating mode were different depending on the type of  $\beta$  subunit. Judging from the fraction of peak current remaining at the end of the test pulse, the most rapidly and slowly inactivating channels in the fast gating mode were those containing the  $\beta_{4a}$  and the  $\beta_{2c}$  subunit, respectively (with intermediate similar values with  $\beta_{3a}$  and  $\beta_{1b}$ ; c.f. also average fraction of inactivating traces in Table II). Judging from the time constant

of inactivation,  $\tau_i$ , obtained from fitting the ensemble averages of the inactivating sweeps (Table II),  $\text{Ca}_v2.1$  channels containing the  $\beta_{4a}$  subunit inactivated more slowly than those containing the  $\beta_{3a}$  or the  $\beta_{1b}$  subunit. The discrepancy may arise in part from the existence and different contribution of an additional noninactivating gating mode of  $\text{Ca}_v2.1$  channels, the b mode, that will be described in the companion paper (Fellin et al., 2004). The different kinetics of inactivation of channels with different  $\beta$  subunits in the slow gating mode could be best appreciated at voltages >30 mV (not depicted).

Also the voltage dependence of steady-state inactivation was different in the two gating modes. Fig. 4 A shows the open probability in successive depolarizations at the same voltage for two representative patches containing a single  $\text{Ca}_v2.1$  ( $\alpha_{1A-2}\beta_{4a}\alpha_{2\delta-1}$ ) channel during recordings in which the holding potential was changed as indicated above the horizontal bars. When the holding potential was changed from -80 to -40 mV, the channel in the slow gating mode did not inactivate, in contrast with the clear inactivation shown by

TABLE II

*Different Properties of Inactivation of Single Human Ca<sub>v</sub>2.1 Channels Containing Different  $\beta$  Subunits in the Fast and Slow Gating Modes*

	$\tau_i$ (ms)	$\%_{in}$	$\%_{in}$	% nulls	% nulls
	fast	fast	slow	fast	slow
$\beta_{1b}$	242	32 ± 8 (6)	7 ± 2 (5)	19 ± 2 (6)	5 ± 1 (5)
$\beta_{2e}$	615	16 ± 5 (11)	2 ± 1 (9)	2 ± 1 (11)	1 ± 1 (9)
$\beta_{3a}$	202	33 ± 11 (5)	ND	4 ± 3 (5)	ND
$\beta_{4a}$	355	60 ± 8 (5)	22 ± 3 (6)	17 ± 5 (5)	9 ± 3 (6)

Single channel recordings as in Fig. 1 on HEK293 cells stably coexpressing human Ca<sub>v</sub>2.1 $\alpha_1$  ( $\alpha_{1A,2}$ ),  $\alpha_{2b}\delta$ -1 and  $\beta_{1b}$ ,  $\beta_{2e}$ ,  $\beta_{3a}$ ,  $\beta_{4a}$  subunits. The time constants of inactivation,  $\tau_i$ , were obtained from fitting the ensemble averages of the inactivating sweeps (pooled averages from the same patches of Fig. 3 B);  $\%_{in}$  represents the average fraction of inactivating sweeps, and % nulls the fraction of traces without activity at a holding potential of -80 mV, obtained from single channel patches (whose number is indicated in parenthesis), in which the channel showed only one gating mode or two clearly separated periods in the two modes. The value of  $\tau_i$  for channels containing the  $\beta_{2e}$  subunit should be considered as a lower limit, because the duration of the depolarizations (720 ms) is too short to define the inactivation kinetic constants. Statistical significance of differences between paired values: for  $\%_{in}$  (slow), all  $\beta$  subunits are significantly different from each other; for  $\%_{in}$  (fast), only  $\beta_{4a}$  is significantly different from all other  $\beta$  subunits ( $P < 0.05$  or  $P < 0.001$ ), probably as a consequence of the large variability in  $\%_{in}$  (fast) among different single channel patches (partly due to different occurrence of a noninactivating gating mode, the b mode, that is described in the companion paper by Fellin et al., 2004). % nulls (fast) with  $\beta_{4a}$  and  $\beta_{1b}$  are both significantly different than those with  $\beta_{2e}$  and  $\beta_{3a}$  ( $P < 0.05$  or  $P < 0.001$ ); for % nulls (slow), the only significant difference is between  $\beta_{4a}$  and  $\beta_{2e}$  ( $P < 0.05$ ). Most of the data for Ca<sub>v</sub>2.1 channels containing the  $\beta_{3a}$  subunit were obtained from PBI-14 cells transfected with  $\beta_{3a}$  cDNA (given the low level of expression of  $\beta_{3a}$  subunit in this stable cell line).

the channel in the fast mode. Steady-state inactivation occurred at more negative voltages in the fast than in the slow gating mode independently of the type of  $\beta$  subunit, as shown in Fig. 4 B for Ca<sub>v</sub>2.1 channels containing either  $\beta_{1b}$  or  $\beta_{4a}$  subunits. However, the voltage dependence of steady-state inactivation in each gating mode depended on the type of  $\beta$  subunit, as shown for the fast gating mode in Fig. 4 C. The average open probabilities at different holding potentials in Fig. 4 (B and C) were obtained by averaging the open probability of all consecutive sweeps at a given holding potential in several experiments like those in Fig. 4 A. In the slow gating mode, like in the fast gating mode, the channels containing the  $\beta_{1b}$  and  $\beta_{4a}$  subunits inactivated at much more negative voltages than those containing the  $\beta_{2e}$  subunit. With the  $\beta_{2e}$  subunit, the open probability of a channel in the slow gating mode could be obtained at several holding potentials only in a single channel patch, and in this case, the channel did not show any steady-state inactivation up to a holding potential of -10 mV (at which voltage, channels containing  $\beta_{1b}$  and  $\beta_{4a}$  subunits in the slow gating mode were largely inactivated). In single channel patches, the fraction of traces without activity at a holding potential of -80 mV (nulls)

was significantly larger for channels gating in the fast than in the slow mode, and, independently of the gating mode, was significantly larger for channels containing a  $\beta_{1b}$  or  $\beta_{4a}$  subunit than for those containing a  $\beta_{2e}$  subunit (Table II).

The relative occurrence of the slow and fast modes of gating of Ca<sub>v</sub>2.1 channels appeared to depend on the type of  $\beta$  subunit. The fraction of time spent by single recombinant Ca<sub>v</sub>2.1 channels in each gating mode was evaluated in patches containing only one channel, whose activity could be recorded for at least 12 min. In each patch, only the first 12 to 16 min of single channel activity were considered, to avoid possible distortions due to different durations of the recording in different patches. Moreover, due to the difficulty of separating with a rigorous criterion individual sweeps with either fast or slow mode activity, only single channel patches in which the channel showed (by visual inspection) only (or mainly) one gating mode or clearly separated long periods in the two gating modes were considered. The classification of the activity in a certain patch or period as either slow or fast gating mode was then based on the open/closed time histograms and/or on the voltage dependence of the open probability. In 168 min of recording (from 11 single channel patches), channels containing the  $\beta_{1b}$  subunit spent 46% of the time in the slow gating mode. A larger fraction of time (58%, in 183 min of recordings from 12 single channel patches) was spent in the slow gating mode by channels containing the  $\beta_{2e}$  subunit. Channels containing the  $\beta_{4a}$  subunit spent most of the time in the slow gating mode (68%, in 117 min of recordings from nine single channel patches). The opposite was true for channels containing the  $\beta_{3a}$  subunit (34%, in 87 min of recordings from six single channel patches). According to Fisher exact test, the differences in occurrence of the fast and slow gating modes among channels with the different  $\beta$  subunits are all statistically significant ( $P < 0.05$  or 0.001). Transitions from the slow gating mode (present at the beginning of the recording) to the fast mode were observed in 2, 3, 0, and 2 single channel patches with the  $\beta_{1b}$ ,  $\beta_{2e}$ ,  $\beta_{3a}$ , and  $\beta_{4a}$  subunit, respectively. The opposite transition from the fast gating mode (present at the beginning) to the slow mode was observed only in one single channel patch with the  $\beta_{4a}$  subunit. In the remaining single channel patches, the channel remained mainly or only in either the fast (5, 3, 4, and 1 patches) or slow gating mode (4, 6, 2, and 5 patches).

In contrast with the gating properties, the permeation properties of Ca<sub>v</sub>2.1 channels were not affected by the type of  $\beta$  subunit. Ca<sub>v</sub>2.1 channels containing the four different  $\beta$  subunits had identical single channel currents and conductances (Fig. 5).

Given the infrequent transitions between the slow and fast modes of gating, and the well established fact

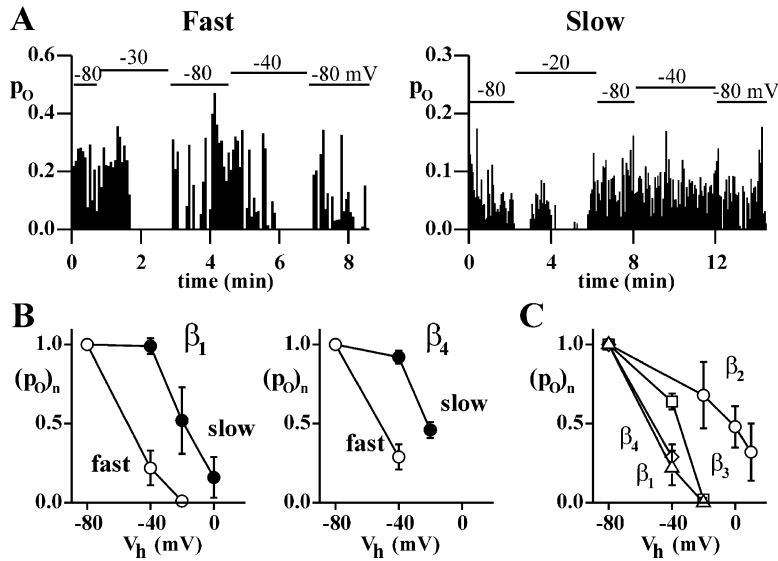


FIGURE 4. Steady-state inactivation of human  $\text{Ca}_v2.1$  channels occurs at more negative voltages in the fast than in the slow gating mode, independently of the  $\beta$  subtype. Single channel recordings as in Fig. 1 on HEK293 cells stably coexpressing human  $\text{Ca}_v2.1\alpha_1$  ( $\alpha_{1A2}$ ),  $\alpha_{2b}\delta-1$ , and  $\beta_{1b}$ ,  $\beta_{2e}$ ,  $\beta_{3a}$ , or  $\beta_{4a}$  subunits. (A) Open probability in successive depolarizations at +30 mV as a function of time during recordings in which the holding potential was changed as indicated above the horizontal bars, from two representative patches containing a single  $\text{Ca}_v2.1$  ( $\alpha_{1A2}-\beta_{4a}-\alpha_{2b}\delta-1$ ) channel in either the fast (left) or the slow gating mode (right). (B) Normalized open probability,  $(p_o)_n$ , at +30 mV of  $\text{Ca}_v2.1$  channels gating in the fast and slow modes containing either the  $\beta_{1b}$  or the  $\beta_{4a}$  subunits as a function of holding potential,  $V_h$ , obtained from patches containing a single channel showing only, or mainly, one gating mode or two clearly separated periods in the two modes.  $P_o$  at different holding potentials was obtained by averaging the open probability of all consecutive sweeps at a given  $V_h$  in experiments ( $n = 3-8$ ) like those in A. In each experiment, the open probability was normalized to the value at  $V_h = -80$  mV. (C) Normalized open probability,  $(p_o)_n$ , at +30 mV of  $\text{Ca}_v2.1$  channels containing different  $\beta$  subunits all gating in the fast mode as a function of  $V_h$ .  $\beta_{1b}$  ( $\Delta$ ),  $\beta_{2e}$  ( $\circ$ ),  $\beta_{3a}$  ( $\square$ ),  $\beta_{4a}$  ( $\diamond$ ). Most of the patches contained a single channel. Part of the data for  $\text{Ca}_v2.1$  channels containing the  $\beta_{2e}$  subunit were obtained from HEK293 cells transiently coexpressing human  $\text{Ca}_v2.1\alpha_1$ ,  $\alpha_{2b}\delta-1$ , and  $\beta_{2e}$  subunits. Most of the data for  $\text{Ca}_v2.1$  channels containing the  $\beta_{3a}$  subunit were obtained from PBI-14 cells transfected with  $\beta_{3a}$  cDNA.

that  $\text{Ca}_v2.1$  channels containing a  $\beta$  subunit activate and inactivate at more negative voltages than channels lacking a  $\beta$  subunit (Stea et al., 1994; De Waard and Campbell, 1995), one might wonder whether the slow gating mode (showing activation and inactivation at more positive voltages than the fast mode) corresponds to channels that have lost the  $\beta$  subunit. This hypothe-

sis is made unlikely by the observation that most of the observed transitions between gating modes were from the slow to the fast mode, and is ruled out by the different properties of inactivation of channels containing different  $\beta$  subunits in the slow gating mode. An additional conclusive evidence against the same hypothesis is the fact that, in HEK293 cells transfected with only  $\text{Ca}_v2.1\alpha_1$  and  $\alpha_{2b}\delta-1$  subunits, single  $\text{Ca}_v2.1$  channels did not gate in the slow gating mode. Interestingly, channels containing only  $\text{Ca}_v2.1\alpha_1$  and  $\alpha_{2b}\delta-1$  subunits showed a low- $p_o$  mode of gating, different from both the fast and the slow gating modes (Figs. 6 and 7).

Fig. 6 shows consecutive traces of activity at +30 mV from a patch containing a single  $\alpha_{1A2}-\alpha_{2b}\delta-1$  channel and the open-closed time histograms and activation curve of the same channel. Fig. 7 compares the gating parameters of the low- $p_o$  mode typical of  $\alpha_{1A2}-\alpha_{2b}\delta-1$  channels with those of the slow and fast gating modes of  $\text{Ca}_v2.1$  channels containing a  $\beta$  subunit. In comparison with the slow and fast gating modes, the low- $p_o$  mode of  $\text{Ca}_v2.1$  channels lacking the  $\beta$  subunit was characterized by shorter open times and longer closed times (Fig. 6, A and B, and Fig. 7 A), by longer first latencies to channel opening (Fig. 7 C), by activation at more positive voltages, lower open probability, and shallower dependence of the open probability on voltage (Fig. 6 C and Fig. 7 B), and by a much larger number of nulls ( $64 \pm 5\%$  out of 578 traces at +30 mV in five single channel patches). The time constants of the two exponential components best fitting the open time histograms were both smaller in the low- $p_o$  gating

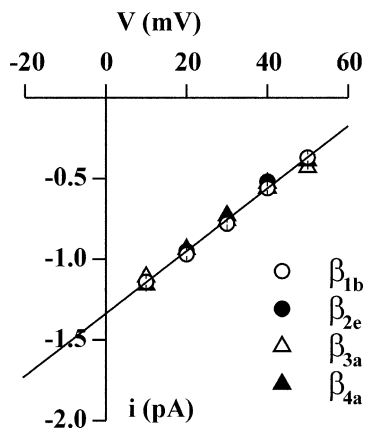


FIGURE 5. The single channel current and conductance of  $\text{Ca}_v2.1$  channels do not depend on the type of  $\beta$  subunit. Single channel recordings as in Fig. 1 on HEK293 cells stably coexpressing human  $\text{Ca}_v2.1\alpha_1$  ( $\alpha_{1A2}$ ),  $\alpha_{2b}\delta-1$ , and  $\beta_{1b}$ ,  $\beta_{2e}$ ,  $\beta_{3a}$ , or  $\beta_{4a}$  subunits. Unitary current,  $i$ , as a function of voltage of  $\text{Ca}_v2.1$  channels containing the  $\beta_{1b}$  ( $\circ$ ),  $\beta_{2e}$  ( $\bullet$ ),  $\beta_{3a}$  ( $\Delta$ ), and  $\beta_{4a}$  ( $\blacktriangle$ ) subunit. The average  $i$ - $V$  relationships were obtained from 5, 6, 4, and 12 patches and the average slope conductance was of  $19.5 \pm 0.4$ ,  $20 \pm 0.4$ ,  $19 \pm 0.9$ , and  $20 \pm 0.4$  pS for channels containing the  $\beta_{1b}$ ,  $\beta_{2e}$ ,  $\beta_{3a}$ , and  $\beta_{4a}$  subunit, respectively.



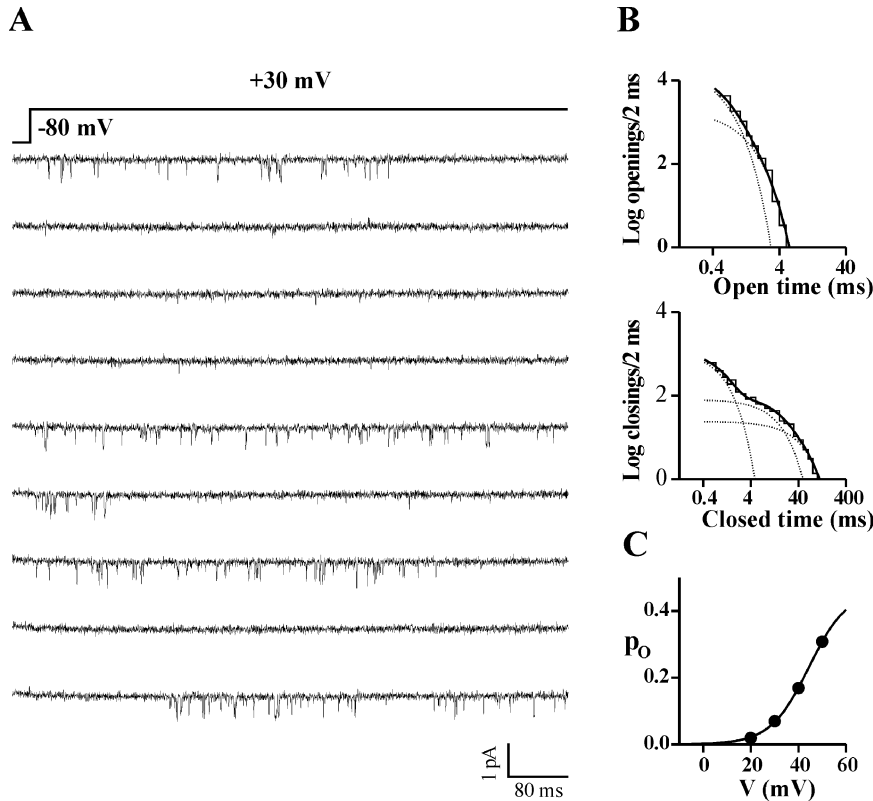


FIGURE 6. The main gating mode of  $Ca_v2.1$  channels lacking the  $\beta$  subunit is a low- $p_o$  mode different from both the fast and the slow gating modes. Single channel recordings as in Fig. 1 on HEK293 cells transiently coexpressing human  $Ca_v2.1\alpha_1$  ( $\alpha_{1A-2}$ ) and  $\alpha_{2b}\delta-1$  subunits. (A) Consecutive traces at +30 mV from a patch containing a single  $\alpha_{1A-2}-\alpha_{2b}\delta-1$  channel. (B) Log-log plots of the open and closed time distributions of the single channel in A. Time constants of the exponential components best fitting the open times: 0.30 and 0.74 ms (relative areas 82 and 18%); time constants for the closed times: 0.69, 11.3, and 34.9 ms (relative areas 31, 36, and 33%). (C) Open probability,  $p_o$ , as a function of voltage for the single channel in A. Fit of the activation curve with a Boltzmann equation gives  $V_{1/2} = 44$  mV,  $k = 9.1$  mV,  $p_{o\max} = 0.46$ .

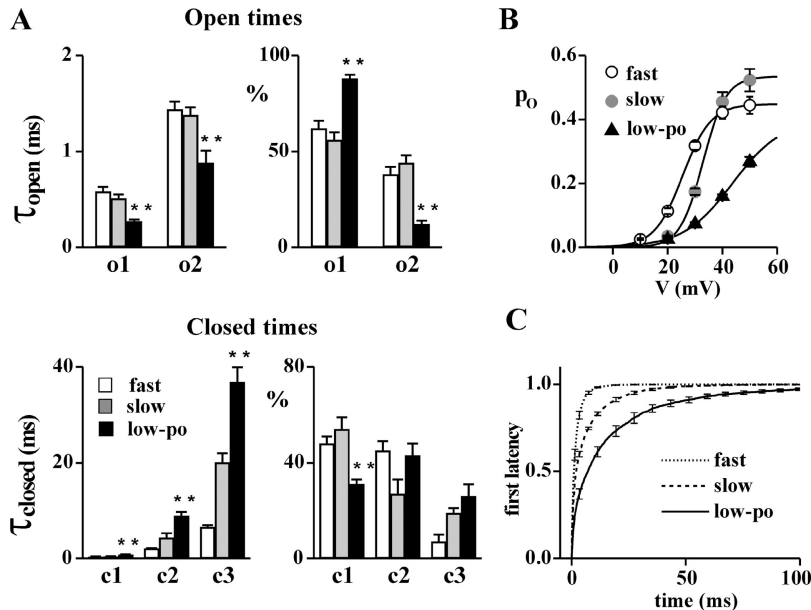


FIGURE 7. Comparison of the gating parameters of the low- $p_o$  gating mode of  $Ca_v2.1$  channels lacking the  $\beta$  subunit and the slow and fast gating modes of  $Ca_v2.1$  channels containing the  $\beta$  subunit. Cell attached recordings on HEK293 cells stably coexpressing human  $\alpha_{1A-2}$ ,  $\alpha_{2b}\delta-1$ , and different  $\beta$  subunits (for the slow and fast gating modes), or transiently expressing  $\alpha_{1A-2}$  and  $\alpha_{2b}\delta-1$  subunits (for the low- $p_o$  gating mode). (A) Time constants ( $\tau_{open}$  and  $\tau_{closed}$ ) and relative areas (%) of the exponential components best fitting the open and closed time distributions at +30 mV of single  $Ca_v2.1$  channels in fast (empty bar), slow (gray bar), and low- $p_o$  (dark bar) gating modes. For the fast and slow gating modes, the values of  $Ca_v2.1$  channels containing different  $\beta$  subunits from 18 (5 with  $\beta_{1b}$ , 3 with  $\beta_{2c}$ , 6 with  $\beta_{3a}$ , and 4 with  $\beta_{4a}$ ) and 13 (5 with  $\beta_{1b}$ , 4 with  $\beta_{2c}$ , and 4 with  $\beta_{4a}$ ) single channel patches, respectively, were averaged; for the low- $p_o$  gating mode, average values were obtained from six patches containing a single  $\alpha_{1A-2}-\alpha_{2b}\delta-1$  channel. Statistical significance of difference between the values for the low- $p_o$  mode and both the slow and fast gating modes, using Student's  $t$  test: \*\*,  $P < 0.001$ . (B) Average open probability as a function of voltage of single  $Ca_v2.1$  channels containing different  $\beta$  subunits in either the fast (open circles,  $n = 18$ ) or the slow (gray circles,  $n = 13$ ) gating mode and of single  $\alpha_{1A-2}-\alpha_{2b}\delta-1$  channels in the low- $p_o$  gating mode (triangles,  $n = 6$ ) as in A. Fit of the activation curves with a Boltzmann equation gives for the low- $p_o$  mode,  $V_{1/2} = 43.6$  mV,  $k = 8.9$  mV,  $p_{o\max} = 0.40$ ; for the fast mode,  $V_{1/2} = 26$  mV,  $k = 5.2$  mV,  $p_{o\max} = 0.45$ ; and for the slow mode,  $V_{1/2} = 33$  mV,  $k = 4.2$  mV,  $p_{o\max} = 0.53$ . The different values of  $p_{o\max}$  for the slow and fast gating modes (in contrast with the similar values in Fig. 1 C) are mainly due to different fractions of time spent by the channels in the b mode (Fellin et al., 2004). (C) Average cumulative first latency histograms of single  $\alpha_{1A-2}-\alpha_{2b}\delta-1$  channels in the low- $p_o$  gating mode (from  $n = 6$  single channel patches) and of single  $\alpha_{1A-2}-\alpha_{2b}\delta-\beta_{1b}$  channels in either the fast or the slow gating mode (from  $n = 5$  and 5 single channel patches, respectively). To obtain the histograms, only sweeps with activity were considered. See text for the parameters of the exponential components best fitting the histograms.

mode and the contribution of the shortest open times was larger; on the other hand, the three closed time constants were all significantly larger and the contribution of the shortest closed times was smaller in the low- $p_o$  gating mode than in both the fast and slow gating modes (Fig. 7 A). As a result, the open probability of the channel in the low- $p_o$  gating mode (at +30 mV) was 0.41 and 0.23 times that in the slow and fast modes, respectively (Fig. 7 B). Fits with a Boltzmann function of the average activation curves of single channels in the three gating modes gave  $V_{1/2}$  (and  $k$ ) values of 44 ( $k = 8.9$ ,  $n = 6$ ) mV, 33 ( $k = 4.2$ ,  $n = 13$ ) mV, and 26 ( $k = 5.2$ ,  $n = 17$ ) mV for the low- $p_o$ , slow, and fast gating modes, respectively (for the latter gating modes, the values from channels containing the different  $\beta$  subunits were averaged together). The cumulative first latency histograms of single  $Ca_v2.1$  channels in both fast and slow gating modes were best fit by the sum of two exponential components ( $\tau_1 = 2.0$  ms, 94%,  $\tau_2 = 8.7$  ms for the fast mode, and  $\tau_1 = 1.8$  ms, 55%,  $\tau_2 = 12$  ms for the slow mode), whereas three exponentials were necessary for the low- $p_o$  mode of  $\alpha_{1A2}$ - $\alpha_{2b}$  $\delta$ -1 channels ( $\tau_1 = 2.3$  ms, 31%,  $\tau_2 = 18$  ms, 59%, and  $\tau_3 = 78$  ms, 10%). The time constant of the fastest component was similar in the three gating modes ( $\sim 2$  ms) but its contribution was very different (from almost 100% for the fast mode, to only 55% and 31% for the slow and low- $p_o$  modes, respectively). Thus,  $Ca_v2.1$  channels in the fast gating mode open more rapidly than those in the slow mode (and the latter more rapidly than those without  $\beta$  subunit in the low- $p_o$  mode).

In addition to the prevailing low- $p_o$  mode of gating,  $Ca_v2.1$  channels containing only  $\alpha_{1A2}$  and  $\alpha_{2b}$  $\delta$ -1 subunits showed a high- $p_o$  mode of gating similar to the fast gating mode of the  $\alpha_{1A2}$ - $\alpha_{2b}$  $\delta$ -1- $\beta$  channels. In three single channel patches, the average open probability at +30 mV of the channel in this gating mode was  $0.267 \pm 0.04$ ; the open time constants were  $0.58 \pm 0.22$  and  $1.4 \pm 0.2$  ms with relative contribution of  $56 \pm 4$  and 44% and the closed time constants were  $0.45 \pm 0.05$ ,  $2.4 \pm 0.1$ , and  $8.8 \pm 1.6$  ms with relative contributions of  $54 \pm 4$ ,  $30 \pm 2$ , and  $16 \pm 2\%$ . The half voltage of activation was  $27 \pm 2$  mV (with  $k = 4.9 \pm 0.2$ ). Much less frequently,  $\alpha_{1A2}$ - $\alpha_{2b}$  $\delta$ -1 channels also showed a mode of gating similar to the slow mode. One may wonder whether the fast and slow gating modes recorded in cells transfected with only  $\alpha_{1A2}$  and  $\alpha_{2b}$  $\delta$ -1 subunits may correspond to channels containing endogenous  $\beta$  subunits (that might be expressed at such low level to be undetectable by Western and Northern blots; Meir et al., 2000). This interpretation appears unlikely in light of the following observation. A low- $p_o$  mode of gating very similar to that just described was the prevailing gating mode present (together with the fast and the rarer slow gating mode) in our initial single channel record-

ings from the cell line PBI-14, which was supposed to stably express  $\alpha_{1A2}$ ,  $\alpha_{2b}$  $\delta$ , and  $\beta_{3a}$  subunits. The low- $p_o$  mode of gating was however totally absent after transfection of PBI-14 cells with  $\beta_{3a}$  cDNA, suggesting that for some reasons these cells were not expressing sufficient amounts of  $\beta_{3a}$  subunits, and therefore most of the recorded single channels lacked the  $\beta_{3a}$  subunit. Indeed, the single channel open probability ( $0.07 \pm 0.01$ ,  $n = 3$ ), the open and closed time constants ( $\tau_{o1} = 0.26 \pm 0.04$  ms,  $\tau_{o2} = 0.97 \pm 0.26$  ms;  $\tau_{c1} = 0.72 \pm 0.10$  ms,  $\tau_{c2} = 8.8 \pm 0.3$  ms,  $\tau_{c3} = 34 \pm 5$  ms,  $n = 3$ ), and the fraction of nulls ( $64 \pm 6\%$ ,  $n = 4$ ) obtained for the low- $p_o$  gating pattern in PBI-14 cells were very similar to those obtained for the low- $p_o$  activity in HEK293 cells transfected with only  $\alpha_{1A2}$  and  $\alpha_{2b}$  $\delta$ -1 subunits. Interestingly, in two single channel patches from PBI-14 cells, transitions of the same channel from the slow to the low- $p_o$  gating mode, and in one of them, from the low- $p_o$  to the fast gating mode and back to the low- $p_o$  mode were observed. This observation is consistent with the hypothesis that the three gating patterns reflect different modes of gating of a  $Ca_v2.1$  channel lacking a  $\beta$  subunit rather than different combinations of  $Ca_v2.1\alpha_1$  subunits and auxiliary subunits. The low- $p_o$  gating mode shown in Figs. 6 and 7 is the prevailing mode of gating of  $Ca_v2.1$  channels without a  $\beta$  subunit, but is completely absent in channels containing a  $\beta$  subunit. In fact, in hundreds of cell-attached patches on HEK293 cells transiently transfected with human  $Ca_v2.1\alpha_1$ ,  $\alpha_{2b}$  $\delta$ -1, and  $\beta_{2e}$  subunits, the low- $p_o$  gating mode was never observed (Hans et al., 1999; Tottene et al., 2002). Likewise, it was never observed in cells transiently transfected with only  $\alpha_{1A2}$  and  $\beta_{2e}$  subunits ( $n = 8$ ).

## DISCUSSION

The main findings reported in this paper can be summarized as follows. (a) Single recombinant human  $Ca_v2.1$  channels show two different modes of gating (slow and fast), characterized by different mean closed times and latency to first opening (both longer when the channel is in the slow mode), different voltage dependence of the open probability (larger depolarizations are necessary to activate the channel in the slow mode), different kinetics of inactivation (slower in the slow mode), and different voltage dependence of steady-state inactivation (occurring at less negative voltages when the channel is in the slow mode). (b)  $Ca_v2.1$  channels containing any of the  $\beta$  subtypes ( $\beta_{1b}$ ,  $\beta_{2e}$ ,  $\beta_{3a}$ , or  $\beta_{4a}$ ) can gate in either the slow or the fast mode, with only minor differences in the rate constants of the transitions between closed and open states within each mode. With all  $\beta$  subunits, inactivation is more rapid and steady-state inactivation occurs at more negative voltages in the fast than in the slow gating mode. However, in both gating modes,  $Ca_v2.1$  channels display dif-

ferent rates of inactivation and different steady-state inactivation depending on the  $\beta$  subtype, with  $\beta_{2e}$  giving a considerably slower rate of inactivation and less negative voltage range of steady-state inactivation than the other  $\beta$  subunits. (c) The relative occurrence of the slow and fast gating modes of  $Ca_v2.1$  channels is modulated by the type of auxiliary  $\beta$  subunit;  $\beta_{3a}$  promotes the fast mode, whereas  $\beta_{4a}$  promotes the slow mode of recombinant  $Ca_v2.1$  channels expressed in HEK293 cells. (d) The prevailing mode of gating of  $Ca_v2.1$  channels lacking a  $\beta$  subunit is a low- $p_o$  mode different from both the fast and the slow gating modes. A channel in the low- $p_o$  mode shows shorter mean open times, longer mean closed times, longer first latency, a much larger fraction of nulls, and activates at more positive voltages, displaying a shallower voltage dependence, than in either the fast or the slow gating mode.

Modal gating appears to be a highly conserved feature among different ion channel types. Discrete modes of single channel activity, presumably corresponding to different sets of protein conformations, have been described for voltage-dependent  $Ca^{2+}$  (Hess and Tsien, 1984; Yue et al., 1990; Plummer and Hess, 1991; Delcour et al., 1993; Forti and Pietrobon, 1993; Rittenhouse and Hess, 1994; Mantegazza et al., 1995),  $Na^+$  (Patlak and Ortiz, 1986; Nilius, 1988; Moorman et al., 1990; Zhou et al., 1991; Alzheimer et al., 1993; Bohle et al., 1998),  $K^+$  (Marrion, 1996; Singer-Lahat et al., 1999), and  $Cl^-$  (Blatz and Magleby, 1986) channels, and also for  $Ca^{2+}$ -activated and G protein-activated  $K^+$  channels (McManus and Magleby, 1988; Smith and Ashford, 1998; Yakubovich et al., 2000) and for ligand-activated channels (for example see Naranjo and Brehm, 1993; Popescu and Auerbach, 2003). In most cases, it remains unclear whether the transitions between modes of gating (occurring in time frames ranging from hundreds of milliseconds to several minutes) reflect slow conformational changes intrinsic to the channels or conformational changes driven by chemical reactions or interaction with other proteins. However, there are several clear instances in which phosphorylation-dephosphorylation reactions either modulate the rate constants of interconversion between different gating modes of the channel or drive the channel into different gating modes corresponding to different states of phosphorylation (c.f. for L-type  $Ca^{2+}$  channels, Ochi and Kawashima, 1990; Yue et al., 1990; Herzig et al., 1993; Ono and Fozzard, 1993; Dzhura et al., 2000; for different  $K^+$  channels, Marrion, 1996; Smith and Ashford, 1998; Singer-Lahat et al., 1999; for a cation channel in *Aplysia* neurons, Wilson and Kaczmarek, 1993). In other cases, it has been shown that the interconversion between different gating modes is either modulated or driven by the interaction of the channel with other proteins, e.g. auxiliary subunits (Naranjo

and Brehm, 1993; Chang et al., 1996; Singer-Lahat et al., 1999; Wakamori et al., 1999; Meir et al., 2000) and/or G protein subunits (Delcour et al., 1993; Lee and Elmslie, 2000; Colecraft et al., 2001), or calmodulin (Imredy and Yue, 1994; Peterson et al., 1999; Zuhlke et al., 1999). In addition, voltage dependence of the rate constants of interconversion between different gating modes has been clearly shown for L-type  $Ca^{2+}$  channels (Pietrobon and Hess, 1990; Forti and Pietrobon, 1993; Cloues et al., 1997; Hivert et al., 1999).

This (and the following, Fellin et al., 2004) is the first report of modal gating of  $Ca_v2.1$  channels. The fast and slow modes of gating, described in this study, are quite different from the gating modes previously reported for L-type and N-type  $Ca^{2+}$  channels (Hess and Tsien, 1984; Yue et al., 1990; Plummer and Hess, 1991; Delcour et al., 1993; Rittenhouse and Hess, 1994; Mantegazza et al., 1995). The distinguishing features are (a) the long mean lifetimes (time frame of several minutes), pointing to quite slow rate constants for the transitions between the two gating modes, and (b) the different kinetics and voltage dependence of inactivation of the channel in the two gating modes, together with different closed times (but similar open times) and different voltage dependence of activation. The gating modes of L-type  $Ca^{2+}$  channels are characterized by large differences in open and closed times of the channel in the different modes, leading to very different open probabilities, without reported clear differences in inactivation properties (Hess and Tsien, 1984; Yue et al., 1990; Mantegazza et al., 1995). Gating modes with different kinetics and voltage dependence of inactivation have been reported for N-type  $Ca^{2+}$  channels (Plummer and Hess, 1991), but the much shorter mean lifetime (few seconds) of the inactivating and noninactivating gating modes of N-type channels and the similar open and closed times of the channel in the two gating modes clearly distinguish the modal behavior of N-type ( $Ca_v2.2$ ) channels from that of  $Ca_v2.1$  channels described here (but see Fellin et al., 2004). On the other hand, inactivating and noninactivating gating modes with mean lifetimes in the time frame of several minutes, which share several properties with the fast and slow gating modes of  $Ca_v2.1$  channels, have been described for  $Na^+$  and  $K_v1.1$  channels (Zhou et al., 1991; Singer-Lahat et al., 1999; Tabarean et al., 1999). For both  $Na^+$  and  $K^+$  channels, there are indirect evidences, from macroscopic current recordings, that interaction of the channel with the cytoskeleton and with  $G\beta\gamma$  subunits either modulate or drive switching between the inactivating and noninactivating gating modes (Levin et al., 1996; Ma et al., 1997; Jing et al., 1999; Tabarean et al., 1999). It will be interesting to investigate with future work whether similar protein interactions modulate or drive switching between the fast

and slow gating modes of  $\text{Ca}_v2.1$  channels. For the time being, we have established that interaction with syntaxin1A is not involved in this mode switching, since incubation with botulinum toxin C1, to cleave syntaxin, did not alter modal gating of human  $\text{Ca}_v2.1$  channels expressed in HEK293 cells (unpublished data; c.f. Sutton et al., 1999).

Our data suggest that the equilibrium between the slow and fast gating modes of  $\text{Ca}_v2.1$  channels is modulated by the type of auxiliary  $\beta$  subunit. Thus,  $\beta$  subunits exert a dual regulation of inactivation of  $\text{Ca}_v2.1$  channels; on one hand, the  $\beta$  subtype affects the inactivation properties of the channel in each gating mode, and, on the other hand, it affects the fraction of time spent by the channel in the slowly inactivating and more rapidly inactivating gating modes. The order of efficiency with which the different  $\beta$  subunits shift the equilibrium between gating modes toward the inactivating fast mode ( $\beta_{3a} > \beta_{1b} > \beta_{2e} > \beta_{4a}$ ) is quite different from that with which they increase the rate of inactivation of the channel ( $\beta_{4a} > \beta_{1b} \cong \beta_{3a} \gg \beta_{2e}$ , judging from the fraction of current inactivating during 720 ms, or  $\beta_{3a} \cong \beta_{1b} > \beta_{4a} \gg \beta_{2e}$ , judging from the time constant of inactivation of the ensemble current of the inactivating traces) or shift steady-state inactivation toward negative voltages ( $\beta_{4a} \cong \beta_{1b} > \beta_{3a} \gg \beta_{2e}$ ). These observations suggest that the  $\beta$  subunit modulation of inactivation properties and of modal gating occurs by different mechanisms and molecular interactions. It might be interesting to note that the two  $\beta$  subunits that seem to favor the slow gating mode are those that specifically interact with the COOH and  $\text{NH}_2$  terminals of the  $\text{Ca}_v2.1\alpha_1$  subunit (Walker et al., 1998, 1999), with  $\beta_{4a}$  showing both a higher affinity for these binding sites and a larger occurrence of the slow gating mode.

The dual independent regulation of channel inactivation by  $\beta$  subunits might contribute to explain the disagreement in the literature regarding the order of efficiencies with which different  $\beta$  subunits modulate the inactivation properties of  $\text{Ca}_v2.1$  channels (Stea et al., 1994; De Waard and Campbell, 1995; Restituito et al., 2000). In fact, different splice variants of  $\text{Ca}_v2.1\alpha_1$  might well display a different equilibrium between the slow and fast gating modes or a different regulation of modal gating by  $\beta$  subunits. Moreover, as found for many channels, mode switching might be modulated by other factors (e.g., interactions with other proteins or metabolic processes) that may be cell type specific.

A large variability of the inactivation properties (both kinetics and voltage range of inactivation) of the whole cell  $\text{Ca}^{2+}$  current in both HEK293 cells and oocytes expressing rat  $\text{Ca}_v2.1$  channels has been reported (Moreno et al., 1997; Restituito et al., 2001; Rousset et al., 2001). A similar variability has been noted also in tsA201 cells expressing  $\text{Ca}_v2.2$  (N-type) channels (Hur-

ley et al., 2000). Restituito et al. (2001) have excluded both different levels of palmitoylation and different levels of  $\beta$  expression as the cause of the variable inactivation properties, and have proposed that the variability may reflect a variable fraction of channels that have lost the  $\beta$  subunit after being targeted to the membrane. Our single channel recordings do not support the presence of a significant fraction of  $\text{Ca}_v2.1$  channels lacking a  $\beta$  subunit in transfected HEK293 cells. In fact, in hundreds of cell-attached patches on cells transiently transfected with human  $\text{Ca}_v2.1\alpha_1$ ,  $\alpha_2\delta$ , and  $\beta_2$  subunits, the low- $p_o$  gating mode, typical of  $\text{Ca}_v2.1$  channels lacking a  $\beta$  subunit, was never observed. On the other hand, a variability in the equilibrium between the gating modes described in this and the companion paper (Fellin et al., 2004) may well explain the variable inactivation properties of recombinant  $\text{Ca}_v2.1$  channels in different cells (c.f. variable fraction of time spent by a single  $\text{Ca}_v2.1$  channel in the different gating modes).

In many central synapses,  $\text{Ca}_v2.1$  channels are preferentially located at the release sites and are more effectively coupled to neurotransmitter release than other  $\text{Ca}^{2+}$  channel types (Mintz et al., 1995; Wu et al., 1999; Qian and Noebels, 2001). At these synapses, the action potential-evoked  $\text{Ca}^{2+}$  influx and the local  $\text{Ca}^{2+}$  increase that triggers neurotransmitter release are mainly determined by the kinetics of opening and closing, the open probability, and the unitary conductance of  $\text{Ca}_v2.1$  channels (Borst and Sakmann, 1998; Sabatini and Regehr, 1999; Meinrenken et al., 2002, 2003). Given the steep dependence of neurotransmitter release on  $\text{Ca}^{2+}$  influx (Dodge and Rahamimoff, 1967; Bollmann et al., 2000; Schneggenburger and Neher, 2000), even small changes in these properties have a large effect on the number of vesicles released by an action potential (Sabatini and Regehr, 1999; Meinrenken et al., 2002). The impact of a relatively small change in the kinetics of activation of presynaptic  $\text{Ca}^{2+}$  channels on the  $\text{Ca}^{2+}$  current and neurotransmitter release evoked by an action potential at a central synapse has been shown by Borst and Sakmann (1998). The presynaptic  $\text{Ca}^{2+}$  channels (mainly P/Q) of the Calyx of Held activated more rapidly after a brief prepulse; the faster activation resulted in an increased action potential-evoked presynaptic  $\text{Ca}^{2+}$  current, which could be simulated with a small increase in the rate constant for gate opening (using a Hodgkin and Huxley-type kinetic scheme to model  $\text{Ca}^{2+}$  channel gating). The importance of the kinetics of activation of presynaptic  $\text{Ca}^{2+}$  channels in determining the fraction of channels that open during a short action potential and the ensuing  $\text{Ca}^{2+}$  current waveform and neurotransmitter release has been shown also by Sabatini and Regehr (1999) with similar simulations.

Human  $\text{Ca}_v2.1$  channels gating in the slow or the fast gating mode have quite different latencies to first open-

ing, activation curves, and open probabilities. The magnitude and timing of  $\text{Ca}^{2+}$  influx in response to an action potential are then expected to be quite different for  $\text{Ca}_v2.1$  channels in the fast or the slow gating mode. One can approximately infer the impact that the different latencies to first opening of channels in the fast and slow mode may have on the  $\text{Ca}^{2+}$  current evoked by an action potential by considering the impact of G protein modulation of  $\text{Ca}_v2.1$  channels on the action potential-evoked  $\text{Ca}^{2+}$  current as measured by Colecraft et al. (2001). The relative difference in latencies to first opening between G protein-inhibited single rat  $\text{Ca}_v2.1$  channels and uninhibited channels in Colecraft et al. (2001) appears in fact comparable to that between human  $\text{Ca}_v2.1$  channels in the slow and fast mode (at nearly equivalent voltages, taking into account that both the  $p_o$ -V and  $i$ -V curves measured by Colecraft et al. appear to be shifted by  $\sim 15$  mV toward positive voltages with respect to those measured here). The longer latency to first opening of G protein-inhibited channels produced a marked reduction of the whole cell  $\text{Ca}^{2+}$  current elicited by an action potential (Colecraft et al., 2001). One can predict that the slow mode of  $\text{Ca}_v2.1$  channels would produce a comparable reduction of the  $\text{Ca}^{2+}$  current elicited by an action potential. Note that the lower open probability of a channel in the slow mode, compared with the fast mode, would also contribute to reduce  $\text{Ca}^{2+}$  influx in response to an action potential.

Synaptic transmission and other physiological responses that are dependent on action potential-evoked  $\text{Ca}^{2+}$  influx through  $\text{Ca}_v2.1$  channels would then be potentially modulated by any factor that regulates the equilibrium between the slow and fast modes of gating of  $\text{Ca}_v2.1$  channels. The auxiliary  $\beta$  subunit appears to be one of these factors since the relative occurrence of the fast and slow gating modes was different in single human  $\text{Ca}_v2.1$  channels containing different  $\beta$  subunits. The  $\beta$  subunit composition of  $\text{Ca}_v2.1$  channels could thus contribute to fine tune presynaptic  $\text{Ca}^{2+}$  influx to local physiological requirements and contribute to create the great diversity of release efficacy at different synapses (Atwood and Karunanithi, 2002). Given the different inactivation properties of the fast and the slow mode and the dual regulation of inactivation of human  $\text{Ca}_v2.1$  channels by  $\beta$  subtypes (affecting both the equilibrium between modes and inactivation within modes),  $\text{Ca}_v2.1$  channels containing different  $\beta$  subunits may also lead to different amounts and timing of  $\text{Ca}^{2+}$  influx in response to presynaptic trains of action potentials (Forsythe et al., 1998) or to postsynaptic complex voltage waveforms (containing both excitatory postsynaptic potentials and action potentials) as those generated in response to high-frequency presynaptic stimulation (Liu et al., 2003). Liu et al. (2003)

have shown that different kinetics of inactivation and especially voltage-dependence of steady-state inactivation of  $\text{Ca}^{2+}$  channels have a striking impact on the amount and temporal pattern of  $\text{Ca}^{2+}$  influx in response to the repetitive firing waveforms that simulate the postsynaptic response of a pyramidal neuron to high-frequency and theta rhythm presynaptic stimulation. The  $\beta$  subunit composition of  $\text{Ca}_v2.1$  channels may therefore also contribute to fine tune postsynaptic  $\text{Ca}^{2+}$  influx and  $\text{Ca}^{2+}$ -dependent processes to specific stimuli and local physiological requirements. It may also contribute to create the great diversity of short-term synaptic plasticity at different synapses (Forsythe et al., 1998; Atwood and Karunanithi, 2002).

As discussed above, modal gating is widespread among channels and regulation of the equilibrium between gating modes appears as a widespread mechanism for neuromodulation of channel function.  $\text{Ca}_v2.1$  channels are known to be regulated by many different transmitters and various signaling pathways (Catterall, 2000; Dolphin, 2003b; Elmslie, 2003). Except for G proteins (Colecraft et al., 2001), modulation of  $\text{Ca}_v2.1$  channels has not been studied at the single channel level. We can exclude that the slow gating mode corresponds to the reluctant gating mode of  $\text{Ca}_v2.1$  channels bound to  $\text{G}\beta\gamma$  (Colecraft et al., 2001). However, a shift in the equilibrium between slow and fast gating modes may be possibly involved in the regulation of  $\text{Ca}_v2.1$  channels by, e.g., phosphatidylinositol-4,5-bisphosphate (Wu et al., 2002), or oxidation (Li et al., 1998; Chen et al., 2002) or hippocampal  $\text{A}_{2b}$  adenosine receptors (Mogul et al., 1993). In each case, at the whole-cell level, the modulation produced changes in the voltage dependence of  $\text{Ca}^{2+}$  current activation. While it remains to be seen whether these changes were due to shifts between the gating modes of  $\text{Ca}_v2.1$  channels, certainly the regulation of the complex modal gating of these channels (described here and in Fellin et al., 2004) provides a potent and versatile mechanism to fine tune  $\text{Ca}^{2+}$  influx and  $\text{Ca}^{2+}$ -dependent processes to specific stimuli in a changing physiological environment. Given the critical role of  $\text{Ca}_v2.1$  channels in controlling neurotransmitter release at central synapses, regulation of their modal gating could have profound consequences on synaptic transmission and plasticity.

The financial support of Telethon-Italy and the Italian Ministry of Education University Research (PRIN, FIRB, ST-L.449/97-CNR-MIUR, FISRL.16/10/2000-CNR-MIUR) to Daniela Pietrobon is gratefully acknowledged.

Olaf S. Andersen served as editor.

Submitted: 3 February 2004

Accepted: 17 September 2004

## REFERENCES

- Alzheimer, C., P.C. Schwindt, and W.E. Crill. 1993. Modal gating of  $\text{Na}^+$  channels as a mechanism of persistent  $\text{Na}^+$  current in pyramidal neurons from rat and cat sensorimotor cortex. *J. Neurosci.* 13:660–673.
- Atwood, H.L., and S. Karunanithi. 2002. Diversification of synaptic strength: presynaptic elements. *Nat. Rev. Neurosci.* 3:497–516.
- Bayliss, D.A., Y.W. Li, and E.M. Talley. 1997. Effects of serotonin on caudal raphe neurons: inhibition of N- and P/Q-type calcium channels and the afterhyperpolarization. *J. Neurophysiol.* 77:1362–1374.
- Bichet, D., V. Cornet, S. Geib, E. Carlier, S. Volsen, T. Hoshi, Y. Mori, and M. De Waard. 2000. The I-II loop of the  $\text{Ca}^{2+}$  channel  $\alpha 1$  subunit contains an endoplasmic reticulum retention signal antagonized by the  $\beta$  subunit. *Neuron.* 25:177–190.
- Bischofberger, J., J.R. Geiger, and P. Jonas. 2002. Timing and efficacy of  $\text{Ca}^{2+}$  channel activation in hippocampal mossy fiber boutons. *J. Neurosci.* 22:10593–10602.
- Blatz, A.L., and K.L. Magleby. 1986. Quantitative description of three modes of activity of fast chloride channels from rat skeletal muscle. *J. Physiol.* 378:141–174.
- Bohle, T., M. Steinbis, C. Biskup, R. Koopmann, and K. Benndorf. 1998. Inactivation of single cardiac  $\text{Na}^+$  channels in three different gating modes. *Biophys. J.* 75:1740–1748.
- Bollmann, J.H., B. Sakmann, and J.G. Borst. 2000. Calcium sensitivity of glutamate release in a calyx-type terminal. *Science.* 289:953–957.
- Borst, J.G., and B. Sakmann. 1998. Facilitation of presynaptic calcium currents in the rat brainstem. *J. Physiol.* 513:149–155.
- Bourinet, E., T.W. Soong, K. Sutton, S. Slaymaker, E. Mathews, A. Monteil, G.W. Zamponi, J. Nargeot, and T.P. Snutch. 1999. Splicing of  $\alpha 1A$  subunit gene generates phenotypic variants of P- and Q-type calcium channels. *Nat. Neurosci.* 2:407–415.
- Brice, N.L., N.S. Berrow, V. Campbell, K.M. Page, K. Brickley, I. Tedder, and A.C. Dolphin. 1997. Importance of the different  $\beta$  subunits in the membrane expression of the  $\alpha 1A$  and  $\alpha 2$  calcium channel subunits: studies using a depolarization-sensitive  $\alpha 1A$  antibody. *Eur. J. Neurosci.* 9:749–759.
- Burgess, D.L., J.M. Jones, M.H. Meisler, and J.L. Noebels. 1997. Mutation of the  $\text{Ca}^{2+}$  channel  $\beta$  subunit gene *Cchb4* is associated with ataxia and seizures in the lethargic (lh) mouse. *Cell.* 88:385–392.
- Burgess, D.L., G.H. Biddlecome, S.I. McDonough, M.E. Diaz, C.A. Zilinski, B.P. Bean, K.P. Campbell, and J.L. Noebels. 1999.  $\beta$  subunit reshuffling modifies N- and P/Q-type  $\text{Ca}^{2+}$  channel subunit compositions in lethargic mouse brain. *Mol. Cell. Neurosci.* 13:293–311.
- Catterall, W.A. 2000. Structure and regulation of voltage-gated  $\text{Ca}^{2+}$  channels. *Annu. Rev. Cell Dev. Biol.* 16:521–555.
- Cens, T., M.E. Mangoni, J. Nargeot, and P. Charnet. 1996. Modulation of the  $\alpha 1A$   $\text{Ca}^{2+}$  channel by  $\beta$  subunits at physiological  $\text{Ca}^{2+}$  concentration. *FEBS Lett.* 391:232–237.
- Chang, S.Y., J. Satin, and H.A. Fozzard. 1996. Modal behavior of the  $\mu 1$   $\text{Na}^+$  channel and effects of coexpression of the  $\beta 1$ -subunit. *Biophys. J.* 70:2581–2592.
- Chen, J., H. Daggett, M. De Waard, S.H. Heinemann, and T. Hoshi. 2002. Nitric oxide augments voltage-gated P/Q-type  $\text{Ca}^{2+}$  channels constituting a putative positive feedback loop. *Free Radic. Biol. Med.* 32:638–649.
- Cloues, R.K., S.J. Tavalin, and N.V. Marrion. 1997.  $\beta$ -Adrenergic stimulation selectively inhibits long-lasting L-type calcium channel facilitation in hippocampal pyramidal neurons. *J. Neurosci.* 17:6493–6503.
- Colecraft, H.M., D.L. Brody, and D.T. Yue. 2001. G-protein inhibition of N- and P/Q-type calcium channels: distinctive elementary mechanisms and their functional impact. *J. Neurosci.* 21:1137–1147.
- Colecraft, H.M., B. Alseikhan, S.X. Takahashi, D. Chaudhuri, S. Mittman, V. Yegnasubramanian, R.S. Alvania, D.C. Johns, E. Marban, and D.T. Yue. 2002. Novel functional properties of  $\text{Ca}^{2+}$  channel  $\beta$  subunits revealed by their expression in adult rat heart cells. *J. Physiol.* 541:435–452.
- Colquhoun, D., and F.J. Sigworth. 1983. Fitting and statistical analysis of single-channel records. In *Single Channel Recordings*. E. Neher, editor. Plenum Publishing Corp., New York. 191–264.
- De Waard, M., and K.P. Campbell. 1995. Subunit regulation of the neuronal  $\alpha 1A$   $\text{Ca}^{2+}$  channel expressed in *Xenopus* oocytes. *J. Physiol.* 485:619–634.
- De Waard, M., D.R. Witcher, M. Pragnell, H. Liu, and K.P. Campbell. 1995. Properties of the  $\alpha 1$ - $\beta$  anchoring site in voltage-dependent  $\text{Ca}^{2+}$  channels. *J. Biol. Chem.* 270:12056–12064.
- Delcour, A.H., D. Lipscombe, and R.W. Tsien. 1993. Multiple modes of N-type calcium channel activity distinguished by differences in gating kinetics. *J. Neurosci.* 13:181–194.
- Dodge, F.A., Jr., and R. Rahamimoff. 1967. Co-operative action a calcium ions in transmitter release at the neuromuscular junction. *J. Physiol.* 193:419–432.
- Dolphin, A.C. 2003a.  $\beta$  subunits of voltage-gated calcium channels. *J. Bioenerg. Biomembr.* 35:599–620.
- Dolphin, A.C. 2003b. G protein modulation of voltage-gated calcium channels. *Pharmacol. Rev.* 55:607–627.
- Dunlap, K., J.I. Luebke, and T.J. Turner. 1995. Exocytotic  $\text{Ca}^{2+}$  channels in mammalian central neurons. *Trends Neurosci.* 18:89–98.
- Dzhura, I., Y. Wu, R.J. Colbran, J.R. Balsler, and M.E. Anderson. 2000. Calmodulin kinase determines calcium-dependent facilitation of L-type calcium channels. *Nat. Cell Biol.* 2:173–177.
- Eilers, J., T. Plant, and A. Konnerth. 1996. Localized calcium signaling and neuronal integration in cerebellar Purkinje neurones. *Cell Calcium.* 20:215–226.
- Elmslie, K.S. 2003. Neurotransmitter modulation of neuronal calcium channels. *J. Bioenerg. Biomembr.* 35:477–489.
- Fellin, T., S. Luvisetto, M. Spagnolo, and D. Pietrobon. 2004. Modal gating of human  $\text{CaV}2.1$  (P/Q-type) calcium channels. II. the b mode and reversible uncoupling from inactivation. *J. Gen. Physiol.* 124:463–474.
- Fletcher, C.F., C.M. Lutz, T.N. O'Sullivan, J.D. Shaughnessy Jr., R. Hawkes, W.N. Frankel, N.G. Copeland, and N.A. Jenkins. 1996. Absence epilepsy in tottering mutant mice is associated with calcium channel defects. *Cell.* 87:607–617.
- Fletcher, C.F., A. Tottene, V.A. Lennon, S.M. Wilson, S.J. Dubel, R. Paylor, D.A. Hosford, L. Tessarollo, M.W. McEnery, D. Pietrobon, et al. 2001. Dystonia and cerebellar atrophy in *Cacna1a* null mice lacking P/Q calcium channel activity. *FASEB J.* 15:1288–1290.
- Forsythe, I.D., T. Tsujimoto, M. Barnes-Davies, M.F. Cuttle, and T. Takahashi. 1998. Inactivation of presynaptic calcium current contributes to synaptic depression at a fast central synapse. *Neuron.* 20:797–807.
- Forti, L., and D. Pietrobon. 1993. Functional diversity of L-type calcium channels in rat cerebellar neurons. *Neuron.* 10:437–450.
- Forti, L., A. Tottene, A. Moretti, and D. Pietrobon. 1994. Three novel types of voltage-dependent calcium channels in rat cerebellar neurons. *J. Neurosci.* 14:5243–5256.
- Hans, M., S. Luvisetto, M.E. Williams, M. Spagnolo, A. Urrutia, A. Tottene, P.F. Brust, E.C. Johnson, M.M. Harpold, K.A. Stauderman, and D. Pietrobon. 1999. Functional consequences of mutations in the human  $\alpha 1A$  calcium channel subunit linked to familial hemiplegic migraine. *J. Neurosci.* 19:1610–1619.
- Helton, T.D., and W.A. Horne. 2002. Alternative splicing of the  $\beta 4$  subunit has  $\alpha 1$  subunit subtype-specific effects on  $\text{Ca}^{2+}$  channel

- gating. *J. Neurosci.* 22:1573–1582.
- Helton, T.D., D.J. Kojetin, J. Cavanagh, and W.A. Horne. 2002. Alternative splicing of a  $\beta 4$  subunit proline-rich motif regulates voltage-dependent gating and toxin block of Cav2.1  $\text{Ca}^{2+}$  channels. *J. Neurosci.* 22:9331–9339.
- Herzig, S., P. Patil, J. Neumann, C.M. Staschen, and D.T. Yue. 1993. Mechanisms of  $\beta$ -adrenergic stimulation of cardiac  $\text{Ca}^{2+}$  channels revealed by discrete-time Markov analysis of slow gating. *Biophys. J.* 65:1599–1612.
- Hess, P., and R.W. Tsien. 1984. Mechanism of ion permeation through calcium channels. *Nature.* 309:453–456.
- Hivert, B., S. Luvisetto, A. Navangione, A. Tottene, and D. Pietrobon. 1999. Anomalous L-type calcium channels of rat spinal motoneurons. *J. Gen. Physiol.* 113:679–694.
- Hurley, J.H., A.L. Cahill, K.P. Currie, and A.P. Fox. 2000. The role of dynamic palmitoylation in  $\text{Ca}^{2+}$  channel inactivation. *Proc. Natl. Acad. Sci. USA.* 97:9293–9298.
- Imredy, J.P., and D.T. Yue. 1994. Mechanism of  $\text{Ca}^{2+}$ -sensitive inactivation of L-type  $\text{Ca}^{2+}$  channels. *Neuron.* 12:1301–1318.
- Jing, J., D. Chikvashvili, D. Singer-Lahat, W.B. Thornhill, E. Reuveny, and I. Lotan. 1999. Fast inactivation of a brain  $\text{K}^{2+}$  channel composed of Kv1.1 and Kv $\beta$ 1.1 subunits modulated by G protein  $\beta \gamma$  subunits. *EMBO J.* 18:1245–1256.
- Jun, K., E.S. Piedras-Renteria, S.M. Smith, D.B. Wheeler, S.B. Lee, T.G. Lee, H. Chin, M.E. Adams, R.H. Scheller, R.W. Tsien, and H.S. Shin. 1999. Ablation of P/Q-type  $\text{Ca}^{2+}$  channel currents, altered synaptic transmission, and progressive ataxia in mice lacking the  $\alpha 1A$ -subunit. *Proc. Natl. Acad. Sci. USA.* 96:15245–15250.
- Krovetz, H.S., T.D. Helton, A.L. Crews, and W.A. Horne. 2000. C-terminal alternative splicing changes the gating properties of a human spinal cord calcium channel  $\alpha 1A$  subunit. *J. Neurosci.* 20:7564–7570.
- Lee, H.K., and K.S. Elmslie. 2000. Reluctant gating of single N-type calcium channels during neurotransmitter-induced inhibition in bullfrog sympathetic neurons. *J. Neurosci.* 20:3115–3128.
- Levin, G., D. Chikvashvili, D. Singer-Lahat, T. Peretz, W.B. Thornhill, and I. Lotan. 1996. Phosphorylation of a  $\text{K}^{+}$  channel  $\alpha$  subunit modulates the inactivation conferred by a  $\beta$  subunit. Involvement of cytoskeleton. *J. Biol. Chem.* 271:29321–29328.
- Li, A., J. Segui, S.H. Heinemann, and T. Hoshi. 1998. Oxidation regulates cloned neuronal voltage-dependent  $\text{Ca}^{2+}$  channels expressed in *Xenopus* oocytes. *J. Neurosci.* 18:6740–6747.
- Liu, H., R. Felix, C.A. Gurnett, M. De Waard, D.R. Witcher, and K.P. Campbell. 1996. Expression and subunit interaction of voltage-dependent  $\text{Ca}^{2+}$  channels in PC12 cells. *J. Neurosci.* 16:7557–7565.
- Liu, Z., J. Ren, and T.H. Murphy. 2003. Decoding of synaptic voltage waveforms by specific classes of recombinant high-threshold  $\text{Ca}^{2+}$  channels. *J. Physiol.* 553:473–488.
- Ludwig, A., V. Flockerzi, and F. Hofmann. 1997. Regional expression and cellular localization of the  $\alpha 1$  and  $\beta$  subunit of high voltage-activated calcium channels in rat brain. *J. Neurosci.* 17:1339–1349.
- Ma, J.Y., W.A. Catterall, and T. Scheuer. 1997. Persistent sodium currents through brain sodium channels induced by G protein  $\beta \gamma$  subunits. *Neuron.* 19:443–452.
- Magee, J., D. Hoffman, C. Colbert, and D. Johnston. 1998. Electrical and calcium signaling in dendrites of hippocampal pyramidal neurons. *Annu. Rev. Physiol.* 60:327–346.
- Mantegazza, M., C. Fasolato, J. Hescheler, and D. Pietrobon. 1995. Stimulation of single L-type calcium channels in rat pituitary GH3 cells by thyrotropin-releasing hormone. *EMBO J.* 14:1075–1083.
- Marrion, N.V. 1996. Calcineurin regulates M channel modal gating in sympathetic neurons. *Neuron.* 16:163–173.
- McCobb, D.P., and K.G. Beam. 1991. Action potential waveform voltage-clamp commands reveal striking differences in calcium entry via low and high voltage-activated calcium channels. *Neuron.* 7:119–127.
- McManus, O.B., A.L. Blatz, and K.L. Magleby. 1987. Sampling, log binning, fitting, and plotting durations of open and shut intervals from single channels and the effects of noise. *Pflugers Arch.* 410:530–553.
- McManus, O.B., and K.L. Magleby. 1988. Kinetic states and modes of single large-conductance calcium-activated potassium channels in cultured rat skeletal muscle. *J. Physiol.* 402:79–120.
- Meinrenken, C.J., J.G. Borst, and B. Sakmann. 2002. Calcium secretion coupling at calyx of held governed by nonuniform channel-vesicle topography. *J. Neurosci.* 22:1648–1667.
- Meinrenken, C.J., J.G. Borst, and B. Sakmann. 2003. Local routes revisited: the space and time dependence of the  $\text{Ca}^{2+}$  signal for phasic transmitter release at the rat calyx of Held. *J. Physiol.* 547:665–689.
- Meir, A., D.C. Bell, G.J. Stephens, K.M. Page, and A.C. Dolphin. 2000. Calcium channel  $\beta$  subunit promotes voltage-dependent modulation of  $\alpha 1B$  by  $G\beta\gamma$ . *Biophys. J.* 79:731–746.
- Mermelstein, P.G., R.C. Foehring, T. Tkatch, W.J. Song, G. Baranauskas, and D.J. Surmeier. 1999. Properties of Q-type calcium channels in neostriatal and cortical neurons are correlated with  $\beta$  subunit expression. *J. Neurosci.* 19:7268–7277.
- Mintz, I.M., V.J. Venema, K.M. Swiderek, T.D. Lee, B.P. Bean, and M.E. Adams. 1992. P-type calcium channels blocked by the spider toxin  $\omega$ -Aga-IVA. *Nature.* 355:827–829.
- Mintz, I.M., B.L. Sabatini, and W.G. Regehr. 1995. Calcium control of transmitter release at a cerebellar synapse. *Neuron.* 15:675–688.
- Mogul, D.J., M.E. Adams, and A.P. Fox. 1993. Differential activation of adenosine receptors decreases N-type but potentiates P-type  $\text{Ca}^{2+}$  current in hippocampal CA3 neurons. *Neuron.* 10:327–334.
- Moorman, J.R., G.E. Kirsch, A.M. Brown, and R.H. Joho. 1990. Changes in sodium channel gating produced by point mutations in a cytoplasmic linker. *Science.* 250:688–691.
- Moreno, H., B. Rudy, and R. Llinas. 1997.  $\beta$  subunits influence the biophysical and pharmacological differences between P- and Q-type calcium currents expressed in a mammalian cell line. *Proc. Natl. Acad. Sci. USA.* 94:14042–14047.
- Mori, Y., M. Wakamori, S. Oda, C.F. Fletcher, N. Sekiguchi, E. Mori, N.G. Copeland, N.A. Jenkins, K. Matsushita, Z. Matsuyama, and K. Imoto. 2000. Reduced voltage sensitivity of activation of P/Q-type  $\text{Ca}^{2+}$  channels is associated with the ataxic mouse mutation rolling Nagoya (tg(rol)). *J. Neurosci.* 20:5654–5662.
- Naranjo, D., and P. Brehm. 1993. Modal shifts in acetylcholine receptor channel gating confer subunit-dependent desensitization. *Science.* 260:1811–1814.
- Nilius, B. 1988. Modal gating behavior of cardiac sodium channels in cell-free membrane patches. *Biophys. J.* 53:857–862.
- Ochi, R., and Y. Kawashima. 1990. Modulation of slow gating process of calcium channels by isoprenaline in guinea-pig ventricular cells. *J. Physiol.* 424:187–204.
- Ono, K., and H.A. Fozzard. 1993. Two phosphatase sites on the  $\text{Ca}^{2+}$  channel affecting different kinetic functions. *J. Physiol.* 470:73–84.
- Ophoff, R.A., G.M. Terwindt, M.N. Vergouwe, R. van Eijk, P.J. Oefner, S.M. Hoffman, J.E. Lamerdin, H.W. Mohrenweiser, D.E. Bulman, M. Ferrari, et al. 1996. Familial hemiplegic migraine and episodic ataxia type-2 are caused by mutations in the  $\text{Ca}^{2+}$  channel gene CACNL1A4. *Cell.* 87:543–552.
- Patlak, J.B., and M. Ortiz. 1986. Two modes of gating during late  $\text{Na}^{+}$  channel currents in frog sartorius muscle. *J. Gen. Physiol.* 87:305–326.

- Peterson, B.Z., C.D. DeMaria, J.P. Adelman, and D.T. Yue. 1999. Calmodulin is the Ca<sup>2+</sup> sensor for Ca<sup>2+</sup>-dependent inactivation of L-type calcium channels. *Neuron*. 22:549–558.
- Pichler, M., T.N. Cassidy, D. Reimer, H. Haase, R. Kraus, D. Ostler, and J. Striessnig. 1997.  $\beta$  subunit heterogeneity in neuronal L-type Ca<sup>2+</sup> channels. *J. Biol. Chem.* 272:13877–13882.
- Pietrobon, D. 2002. Calcium channels and channelopathies of the central nervous system. *Mol. Neurobiol.* 25:31–50.
- Pietrobon, D., and P. Hess. 1990. Novel mechanism of voltage-dependent gating in L-type calcium channels. *Nature*. 346:651–655.
- Pineda, J.C., R.S. Waters, and R.C. Foehring. 1998. Specificity in the interaction of HVA Ca<sup>2+</sup> channel types with Ca<sup>2+</sup>-dependent AHPs and firing behavior in neocortical pyramidal neurons. *J. Neurophysiol.* 79:2522–2534.
- Plummer, M.R., and P. Hess. 1991. Reversible uncoupling of inactivation in N-type calcium channels. *Nature*. 351:657–659.
- Popescu, G., and A. Auerbach. 2003. Modal gating of NMDA receptors and the shape of their synaptic response. *Nat. Neurosci.* 6:476–483.
- Qian, J., and J.L. Noebels. 2001. Presynaptic Ca<sup>2+</sup> channels and neurotransmitter release at the terminal of a mouse cortical neuron. *J. Neurosci.* 21:3721–3728.
- Randall, A., and R.W. Tsien. 1995. Pharmacological dissection of multiple types of Ca<sup>2+</sup> channel currents in rat cerebellar granule neurons. *J. Neurosci.* 15:2995–3012.
- Rao, C.R. 1973. Linear statistical inference and its application. John Wiley & Sons, New York. 400 pp.
- Restituito, S., T. Cens, C. Barrere, S. Geib, S. Galas, M. De Waard, and P. Charnet. 2000. The  $\beta$ 2a subunit is a molecular groom for the Ca<sup>2+</sup> channel inactivation gate. *J. Neurosci.* 20:9046–9052.
- Restituito, S., T. Cens, M. Rousset, and P. Charnet. 2001. Ca<sup>2+</sup> channel inactivation heterogeneity reveals physiological unbinding of auxiliary  $\beta$  subunits. *Biophys. J.* 81:89–96.
- Rittenhouse, A.R., and P. Hess. 1994. Microscopic heterogeneity in unitary N-type calcium currents in rat sympathetic neurons. *J. Physiol.* 474:87–99.
- Rousset, M., T. Cens, S. Restituito, C. Barrere, J.L. Black III, M.W. McEnery, and P. Charnet. 2001. Functional roles of  $\gamma$ 2,  $\gamma$ 3, and  $\gamma$ 4, three new Ca<sup>2+</sup> channel subunits, in P/Q-type Ca<sup>2+</sup> channel expressed in *Xenopus* oocytes. *J. Physiol.* 532:583–593.
- Sabatini, B.L., and W.G. Regehr. 1999. Timing of synaptic transmission. *Annu. Rev. Physiol.* 61:521–542.
- Sandoz, G., D. Bichet, V. Cornet, Y. Mori, R. Felix, and M. De Waard. 2001. Distinct properties and differential  $\beta$  subunit regulation of two C-terminal isoforms of the P/Q-type Ca<sup>2+</sup>-channel  $\alpha$ 1A subunit. *Eur. J. Neurosci.* 14:987–997.
- Sather, W.A., T. Tanabe, J.F. Zhang, Y. Mori, M.E. Adams, and R.W. Tsien. 1993. Distinctive biophysical and pharmacological properties of class A (BI) calcium channel  $\alpha$ 1 subunits. *Neuron*. 11:291–303.
- Schneggenburger, R., and E. Neher. 2000. Intracellular calcium dependence of transmitter release rates at a fast central synapse. *Nature*. 406:889–893.
- Sigworth, F.J., and S.M. Sine. 1987. Data transformations for improved display and fitting of single-channel dwell time histograms. *Biophys. J.* 52:1047–1054.
- Singer-Lahat, D., N. Dascal, and I. Lotan. 1999. Modal behavior of the Kv1.1 channel conferred by the Kv $\beta$ 1.1 subunit and its regulation by dephosphorylation of Kv1.1. *Pflugers Arch.* 439:18–26.
- Smith, M.A., and M.L. Ashford. 1998. Mode switching characterizes the activity of large conductance potassium channels recorded from rat cortical fused nerve terminals. *J. Physiol.* 513:733–747.
- Sokolov, S., R.G. Weiss, E.N. Timin, and S. Hering. 2000. Modulation of slow inactivation in class A Ca<sup>2+</sup> channels by  $\beta$ -subunits. *J. Physiol.* 527:445–454.
- Stea, A., W.J. Tomlinson, T.W. Soong, E. Bourinet, S.J. Dubel, S.R. Vincent, and T.P. Snutch. 1994. Localization and functional properties of a rat brain  $\alpha$ 1A calcium channel reflect similarities to neuronal Q- and P-type channels. *Proc. Natl. Acad. Sci. USA*. 91:10576–10580.
- Sutton, K.G., J.E. McRory, H. Guthrie, T.H. Murphy, and T.P. Snutch. 1999. P/Q-type calcium channels mediate the activity-dependent feedback of syntaxin-1A. *Nature*. 401:800–804.
- Tabarean, I.V., P. Juranka, and C.E. Morris. 1999. Membrane stretch affects gating modes of a skeletal muscle sodium channel. *Biophys. J.* 77:758–774.
- Tanaka, O., H. Sakagami, and H. Kondo. 1995. Localization of mRNAs of voltage-dependent Ca<sup>2+</sup>-channels: four subtypes of  $\alpha$ 1- and  $\beta$ -subunits in developing and mature rat brain. *Brain Res. Mol. Brain Res.* 30:1–16.
- Tottene, A., A. Moretti, and D. Pietrobon. 1996. Functional diversity of P-type and R-type calcium channels in rat cerebellar neurons. *J. Neurosci.* 16:6353–6363.
- Tottene, A., T. Fellin, S. Pagnutti, S. Luvisetto, J. Striessnig, C. Fletcher, and D. Pietrobon. 2002. Familial hemiplegic migraine mutations increase Ca<sup>2+</sup> influx through single human CaV2.1 channels and decrease maximal CaV2.1 current density in neurons. *Proc. Natl. Acad. Sci. USA*. 99:13284–13289.
- Tsunemi, T., H. Saegusa, K. Ishikawa, S. Nagayama, T. Murakoshi, H. Mizusawa, and T. Tanabe. 2002. Novel Cav2.1 splice variants isolated from Purkinje cells do not generate P-type Ca<sup>2+</sup> current. *J. Biol. Chem.* 277:7214–7221.
- Usovicz, M.M., M. Sugimori, B. Cherksey, and R. Llinas. 1992. P-type calcium channels in the somata and dendrites of adult cerebellar Purkinje cells. *Neuron*. 9:1185–1199.
- Vance, C.L., C.M. Begg, W.L. Lee, H. Haase, T.D. Copeland, and M.W. McEnery. 1998. Differential expression and association of calcium channel  $\alpha$ 1B and  $\beta$  subunits during rat brain ontogeny. *J. Biol. Chem.* 273:14495–14502.
- van den Maagdenberg, A.M., D. Pietrobon, T. Pizzorusso, S. Kaja, L.A. Broos, T. Cesetti, R.C. van de Ven, A. Tottene, J. van der Kaa, J.J. Plomp, et al. 2004. Cacna1a knockin migraine mouse model with increased susceptibility to cortical spreading depression. *Neuron*. 41:701–710.
- Volsen, S.G., N.C. Day, A.L. McCormack, W. Smith, P.J. Craig, R. Beattie, P.G. Ince, P.J. Shaw, S.B. Ellis, A. Gillespie, et al. 1995. The expression of neuronal voltage-dependent calcium channels in human cerebellum. *Brain Res. Mol. Brain Res.* 34:271–282.
- Volsen, S.G., N.C. Day, A.L. McCormack, W. Smith, P.J. Craig, R.E. Beattie, D. Smith, P.G. Ince, P.J. Shaw, S.B. Ellis, et al. 1997. The expression of voltage-dependent calcium channel  $\beta$  subunits in human cerebellum. *Neuroscience*. 80:161–174.
- Wakamori, M., G. Mikala, and Y. Mori. 1999. Auxiliary subunits operate as a molecular switch in determining gating behaviour of the unitary N-type Ca<sup>2+</sup> channel current in *Xenopus* oocytes. *J. Physiol.* 517:659–672.
- Walker, D., D. Bichet, K.P. Campbell, and M. De Waard. 1998. A  $\beta$ 4 isoform-specific interaction site in the carboxyl-terminal region of the voltage-dependent Ca<sup>2+</sup> channel  $\alpha$ 1A subunit. *J. Biol. Chem.* 273:2361–2367.
- Walker, D., D. Bichet, S. Geib, E. Mori, V. Cornet, T.P. Snutch, Y. Mori, and M. De Waard. 1999. A new  $\beta$  subtype-specific interaction in  $\alpha$ 1A subunit controls P/Q-type Ca<sup>2+</sup> channel activation. *J. Biol. Chem.* 274:12383–12390.
- Westenbroek, R.E., T. Sakurai, E.M. Elliott, J.W. Hell, T.V. Starr, T.P. Snutch, and W.A. Catterall. 1995. Immunohistochemical identification and subcellular distribution of the  $\alpha$ 1A subunits of brain calcium channels. *J. Neurosci.* 15:6403–6418.
- Wilson, G.F., and L.K. Kaczmarek. 1993. Mode-switching of a voltage-gated cation channel is mediated by a protein kinase A-regu-



- lated tyrosine phosphatase. *Nature*. 366:433–438.
- Witcher, D.R., M. De Waard, H. Liu, M. Pragnell, and K.P. Campbell. 1995. Association of native Ca<sup>2+</sup> channel  $\beta$  subunits with the  $\alpha$ 1 subunit interaction domain. *J. Biol. Chem.* 270:18088–18093.
- Wu, L., C.S. Bauer, X.G. Zhen, C. Xie, and J. Yang. 2002. Dual regulation of voltage-gated calcium channels by PtdIns(4,5)P<sub>2</sub>. *Nature*. 419:947–952.
- Wu, L.G., R.E. Westenbroek, J.G. Borst, W.A. Catterall, and B. Sakmann. 1999. Calcium channel types with distinct presynaptic localization couple differentially to transmitter release in single calyx-type synapses. *J. Neurosci.* 19:726–736.
- Yakubovich, D., V. Pastushenko, A. Bitler, C.W. Dessauer, and N. Dascal. 2000. Slow modal gating of single G protein-activated K<sup>+</sup> channels expressed in *Xenopus* oocytes. *J. Physiol.* 524:737–755.
- Yatani, A., A. Bahinski, G. Mikala, S. Yamamoto, and A. Schwartz. 1994. Single amino acid substitutions within the ion permeation pathway alter single-channel conductance of the human L-type cardiac Ca<sup>2+</sup> channel. *Circ. Res.* 75:315–323.
- Yue, D.T., P.H. Backx, and J.P. Imreedy. 1990. Calcium-sensitive inactivation in the gating of single calcium channels. *Science*. 250:1735–1738.
- Zhou, J.Y., J.F. Potts, J.S. Trimmer, W.S. Agnew, and F.J. Sigworth. 1991. Multiple gating modes and the effect of modulating factors on the  $\mu$ I sodium channel. *Neuron*. 7:775–785.
- Zhuchenko, O., J. Bailey, P. Bonnen, T. Ashizawa, D.W. Stockton, C. Amos, W.B. Dobyns, S.H. Subramony, H.Y. Zoghbi, and C.C. Lee. 1997. Autosomal dominant cerebellar ataxia (SCA6) associated with small polyglutamine expansions in the  $\alpha$ 1A-voltage-dependent calcium channel. *Nat. Genet.* 15:62–69.
- Zuhlke, R.D., G.S. Pitt, K. Deisseroth, R.W. Tsien, and H. Reuter. 1999. Calmodulin supports both inactivation and facilitation of L-type calcium channels. *Nature*. 399:159–162.